UNCLASSIFIED

AD NUMBER

AD011504

NEW LIMITATION CHANGE

TO

Approved for public release, distribution unlimited

FROM

Distribution authorized to U.S. Gov't. agencies and their contractors; Administrative/Operational Use; 15 MAY 1953. Other requests shall be referred to Office of Naval Research, Arlington, VA 22203.

AUTHORITY

ONR ltr dtd 26 Oct 1977

THIS PAGE IS UNCLASSIFIED

AD-
11504

UNCLASSIFIED

Incipient-Cavitation Scaling Experiments

for

Hemispherical and 1.5-Caliber Ogive-Nosed Bodies

A Joint Study by

The Hydrodynamics Laboratory
California Institute of Technology

and

Ordnance Research Laboratory
The Pennsylvania State College

May 15, 1953

Serial No. NOrd 7958-264

Copy No. 31

Department of the Navy

Office of Naval Research
Contract Nonr-24435 NR 062-124

Bureau of Ordnance
Contract NOrd-7958

Incipient-Cavitation Scaling Experiments

for

Hemispherical and 1.5-Caliber Ogive-Nosed Bodies

A Joint Study by

The Hydrodynamics Laboratory
California Institute of Technology

and

Ordnance Research Laboratory
The Pennsylvania State College

May 15, 1953

By

Blaine R. Parkin

J. W. Holl

Approved for Distribution

J. M. Robertson

Assistant Director
Ordnance Research Laboratory
The Pennsylvania State College

M. S. Plesset

The Hydrodynamics Laboratory
California Institute of Technology

Distribution List

Chief, Bureau of Ordnance (Re6) — 2 copies
Department of the Navy
Washington 25, D. C.

Chief, Bureau of Ordnance (Ad3) — 2 copies
Department of the Navy
Washington 25, D. C.

British Joint Services Mission (Navy Staff) — 3 copies
Room 4930, Main Navy Building
18th & Constitution Avenue
Washington 25, D. C.

Via: Bureau of Ordnance (Ad8)
Department of the Navy
Washington 25, D. C.

Commander — 1 copy
U. S. Naval Ordnance Test Station, Inyokern
China Lake, California

Commander — 1 copy
U. S. Naval Ordnance Test Station
3202 East Foothill
Pasadena Activity
Pasadena 8, California

Director, Ordnance Research Laboratory — 1 copy
Pennsylvania State College
State College, Pennsylvania

Via: Development Contract Administrator
Ordnance Research Laboratory
Pennsylvania State College
State College, Pennsylvania

Commander — 2 copies
U. S. Naval Ordnance Laboratory
White Oak
Silver Spring 19, Maryland

Commanding Officer — 2 copies
U. S. Naval Underwater Ordnance Station
Newport, Rhode Island

Director, Applied Physics Laboratory — 1 copy
University of Washington
Seattle, Washington

Via: Inspector of Naval Material
412 Lyon Building
607 Third Avenue
Seattle 4, Washington

Commanding Officer and Director — 1 copy
David Taylor Model Basin
Carderock, Maryland

Chief of Naval Research — 1 copy
Department of the Navy
Washington 25, D. C.

Director — 1 copy
U. S. Naval Research Laboratory
Washington 25, D. C.

Chief of Naval Operations (OP 316) — 1 copy
Department of the Navy
Washington 25, D. C.

General Electric Company — 1 copy
Pittsfield, Massachusetts

Via: Naval Inspector of Ordnance
Schenectady, New York

General Electric Company — 1 copy
Schenectady, New York

Via: Naval Inspector of Ordnance
Schenectady, New York

Westinghouse Electric Corporation — 1 copy
Sharon, Pennsylvania

Via: Development Contract Administrator
Westinghouse Electric Corporation
Sharon, Pennsylvania

Aerojet Corporation — 1 copy
Azusa, California

Via: Bureau of Aeronautics Representative
15 South Raymond Street
Pasadena, California

National Advisory Committee for Aeronautics — 1 copy
1724 "F" Street, N. W.
Washington, D. C.

Director, Experimental Towing Tank — 1 copy
Stevens Institute of Technology
711 Hudson Street
Hoboken, New Jersey

Via: Inspector of Naval Material
Naval Industrial Reserve Shipyard
Building 13
Port Newark, New Jersey

Director, Hydrodynamics Laboratory — 1 copy
California Institute of Technology
Pasadena, California

Via: Inspector of Naval Material
1206 South Santee Street
Los Angeles 15, California

Chief, Bureau of Ships — 1 copy
Department of the Navy
Washington 25, D. C.

Chief, Bureau of Aeronautics — 1 copy
Department of the Navy
Washington 25, D. C.

Johns Hopkins University — 1 copy
(Mr. Wiaclencinus)
Baltimore, Maryland

Via: Inspector of Naval Material
401 Water Street
Baltimore 2, Maryland

Brush Development Company — 1 copy
3405 Perkins Avenue
Cleveland 14, Ohio

Via: Inspector of Naval Material
1620 Euclid Avenue, 3rd Floor
Cleveland 15, Ohio

Chief of Naval Research — 2 copies
c/o Technical Information Division
Library of Congress
Washington 25, D. C.

University of Minnesota — 1 copy
Hydrodynamics Laboratory
Minneapolis, Minnesota

Hydrodynamics Laboratory — 1 copy
Massachusetts Institute of Technology
Cambridge, Massachusetts

Illinois Institute of Technology — 1 copy
Chicago, Illinois

Physics Department — 1 copy
(Mr. Lindsay)
Brown University
Providence, Rhode Island

DISTRIBUTION LIST CONTINUED
(Contract N6onr-24435)

Chief of Naval Research (N482) — 11 copies
Office of Naval Research
Department of the Navy
Washington 25, D. C.

Director, Office of Naval Research — 1 copy
Boston Branch
495 Summer Street
Boston 10, Massachusetts

Director, Office of Naval Research — 2 copies
346 Broadway
New York 13, New York

Office of Naval Research — 2 copies
London Branch
Office of Asst. Naval Attache for Research
American Embassy, Navy 100
Fleet Post Office
New York, New York

Director, Office of Naval Research — 2 copies
Los Angeles Branch
1030 East Green Street
Pasadena 1, California

Director, Office of Naval Research — 1 copy
San Francisco Branch
801 Donahue Street
San Francisco 24, California

Director, Office of Naval Research — 1 copy
Chicago Branch
American Fore Building
844 North Rush Street
Chicago 11, Illinois

Aerojet Engineering Corporation — 1 copy
332 North Irwindale Road
Azusa, California
Attention: C. Gongwer

Commander, Naval Ordnance Test Station, Inyokern — 1 copy
China Lake, California
Attention: Technical Library, Code 5507

Officer-in-Charge, Pasadena Annex — 2 copies
Naval Ordnance Test Station, Inyokern
3202 East Foothill Boulevard
Pasadena, California
Attention: Pasadena Annex Library, Code P5507

Commander, Submarine Development Group Two — 1 copy
Box 70, U. S. Naval Submarine Base
New London, Connecticut

Dr. F. C. Lindvall — 1 copy
California Institute of Technology
1201 East California Street
Pasadena 4, California

Abstract

THIS REPORT presents the results of the joint experimental program on cavitation scale effects conducted at the Ordnance Research Laboratory, The Pennsylvania State College, and the Hydrodynamics Laboratory, California Institute of Technology. Two families of axially symmetric bodies were tested in the Garfield Thomas Water Tunnel at ORL and in the High-Speed Water Tunnel at CIT. One family of bodies consisted of models with hemispherical noses while the other geometrically similar family had 1.5-caliber ogive noses.

It was found that in spite of differences in the test facilities, such as the resorber in the High-Speed Water Tunnel circuit, the measurements for incipient cavitation taken at CIT and ORL showed good agreement. The dependence of the incipient cavitation number upon free-stream velocity and model size, previously observed at CIT, was verified. In addition, the range of model sizes was extended to larger scale for the ORL experiments. It was found that the values for the incipient cavitation number for each family of models could be represented as a function of the product of the flow velocity and the square root of the model size. These results show that for cavitation tests of small models it is not correct to assume that the incipient cavitation number equals the negative of the minimum pressure coefficient.

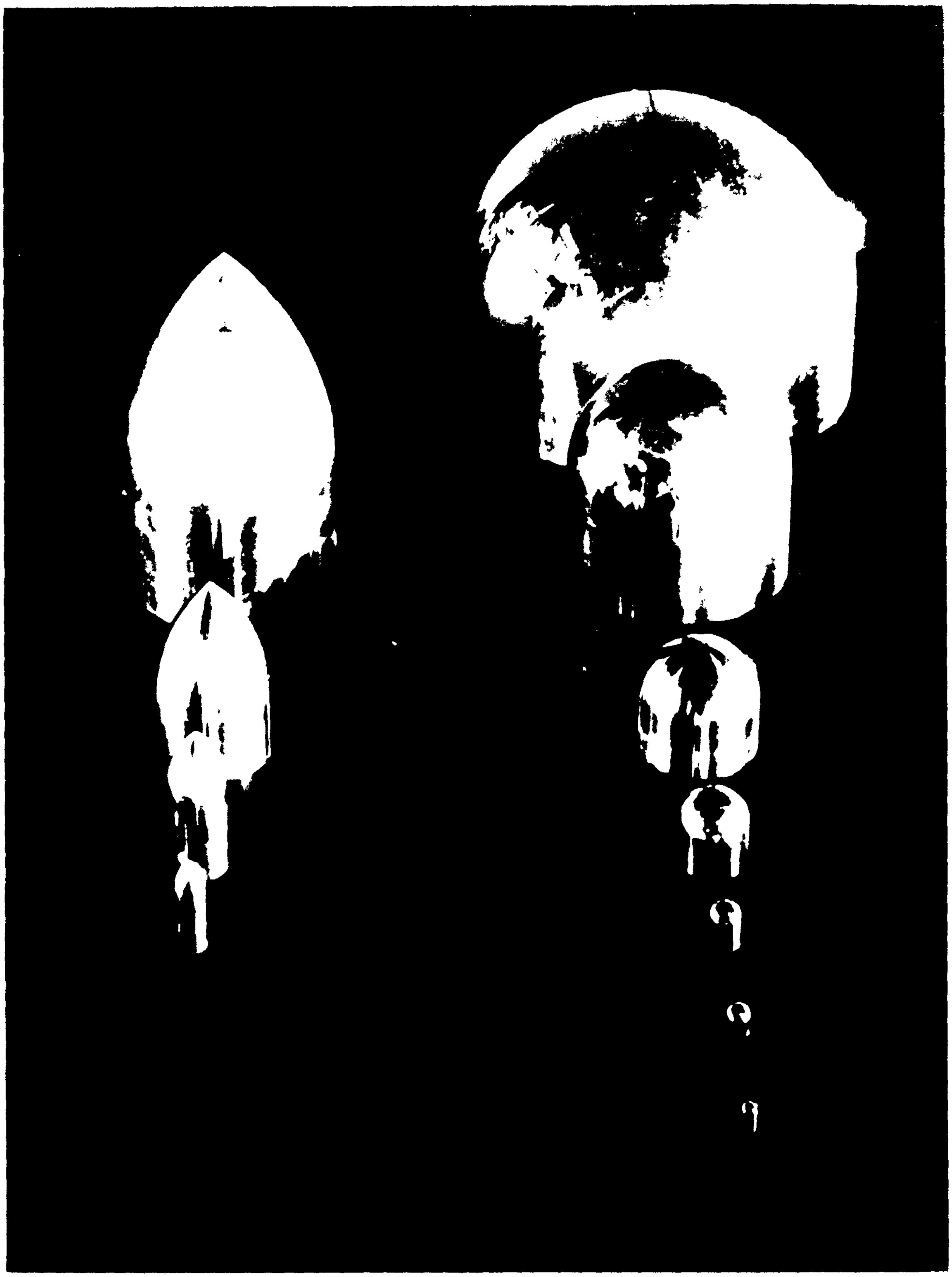

Contents

Illustrations

Introduction

EXPERIMENTS at the Hydrodynamics Laboratory, California Institute of Technology[1,2*], have shown that the inception of cavitation on geometrically similar bodies in steady rectilinear liquid flow is definitely influenced by the size of the body and the free-stream velocity. Further, it has been found theoretically that if Reynolds-number effects are neglected, the inception of cavitation still depends upon both free-stream velocity and model size[3]. For the experiments performed at CIT, the largest body in any geometrically similar family of axially symmetric models was two inches in diameter. Consequently, it was desirable to extend the range to larger sizes. Further, no other laboratory had attempted to confirm the trends observed at CIT. Therefore, the Ordnance Research Laboratory at The Pennsylvania State College and the Hydrodynamics Laboratory at CIT have been cooperating in a joint research program to extend observations of incipient cavitation to larger models and to compare the results obtained when a given series of models is tested in two different test facilities. This report presents the results of the joint research program which was carried out in the 14-inch High-Speed Water Tunnel of the Hydrodynamics Laboratory, CIT, and the 48-inch Garfield Thomas Water Tunnel at ORL.

Throughout this report we shall use the term "incipient cavitation number", σ, to designate that state of liquid flow in which cavitation disappears as the static pressure is slowly increased at constant free-stream velocity.** We shall also include that state in which small wisps of cavitation occur only intermittently near the point of lowest pressure on the model. This definition is only one of several ways by which the inception conditions could be determined. For example, it might seem more logical to require that the pressure be lowered from the noncavitating flow state to determine incipient cavitation. However, experience has shown that the present definition enables one to obtain reproducible data for that flow state at the highest free-stream static pressure for which cavitation can occur at a given velocity on smooth bodies. If the pressure is lowered to this value, cavitation may or may not occur, and its occurrence depends in a random manner upon the time during which the pressure is held at the lower value. Thus, the present definition offers the engineering advantage that conservative values can be found, and it simplifies the problem by excluding any time dependence as well as giving reproducible experimental results. We use the customary definition for the cavitation number, σ, namely,

$$\sigma = \frac{p_0 - p_v}{\frac{1}{2}\rho V_0^2}$$

where p_0 is the free-stream static pressure, p_v is the liquid vapor pressure, ρ is the liquid density, and V_0 is the free-stream velocity.

In this investigation we have confined ourselves to determining visually the incipient cavitation number of two families of geometrically similar axially symmetric bodies in steady rectilinear flows at various free-stream velocities and at several values of dissolved-air content. The two model shapes consist of right circular cylindrical bodies with hemispherical noses for one family and with 1.5-caliber ogive noses for the other family. The family of hemispheres includes models 1/4, 3/8, 1/2, 1-1/8, 2, 4 and 8 inches in diameter while the family of 1.5-caliber ogives includes models 1/2, 1, 2 and 4 inches in diameter. Except for the four- and eight-inch models, the hemispheres were among those tested by Kermeen[2] at CIT. More detailed descriptions of the models and the test arrangements are given in Appendix A of this report.

* Superscribed numbers refer to the list of references.

** Kermeen[2] calls this flow state "intermittent incipient cavitation".

Test Procedure

The general test procedures for the tests at ORL and CIT were essentially the same for all models. The tunnel velocity was held constant and the free-stream static pressure was lowered until cavitation was established around the entire nose. The pressure was then raised until incipient cavitation was seen to exist (usually on top of the model near the lowest-pressure point). The free-stream static pressure measurement was then recorded and free-stream velocity readings were taken in terms of the pressure differentials across the water-tunnel nozzles. At both CIT and ORL, tunnel pressure fluctuations caused the conditions for incipient cavitation to be unsteady. The test conditions at ORL, and occasionally at CIT, would change from too much cavitation to incipient cavitation and then to no cavitation. The entire cycle repeated itself in various orders. At CIT, where the fluctuations were less severe, a random pressure rise would often cause the incipient cavitation to vanish. The cavitation would not return even though the pressure would fall again to a low value, so that cavitation had to be completely re-established. Therefore, it was necessary to correlate the inception conditions with the static pressure readings by recording only those static pressure readings which were observed when incipient cavitation was seen on the body. The methods used for measuring the free-stream velocity were slightly different at the two laboratories. At ORL, sequences of differential pressure readings were recorded during every observation period. These pressure differences were then averaged so that an average velocity could be calculated for each period when incipient cavitation observations were made. At CIT, the differential pressures were averaged in this way only for tunnel speeds in excess of 60 fps. For lower velocities, the static and differential pressure readings were taken simultaneously when incipient cavitation was seen on the model.

During the ORL experiments, each observer noted the cavitation condition at each velocity. Thus at least two points were obtained for each velocity and a check was made on "personal constants" for identifying incipient cavitation. In practically all cases the two readings agreed very closely. For those models and velocities where very low working-section pressures were required, air came out of solution and the resulting entrained air obscured the model and made data impossible to obtain if the very low static pressure was held for too long a time. This difficulty was overcome by making a measurement as quickly as possible after the free-stream static pressure had been lowered. Then the working-section pressure would be raised to 40 psia and held there for ten minutes to redissolve the entrained air before another reading was taken. It was usually at the end of these high-pressure periods that water samples were collected for a Van Slyke analysis of the dissolved air concentration. In addition to the sample which was taken from the nozzle section, samples were sometimes also taken from the diffuser section and the lower leg of the tunnel. This procedure was followed to check the homogeneity of the water samples. The air-content readings of such triple samples were found to agree within five per cent.

At CIT, the resorber[4] in the High-Speed Water Tunnel circuit allows for continuous operation without appreciable air entrainment so that special techniques were not required. The determinations of air content, with a Van Slyke apparatus, for the CIT experiments followed the procedure outlined by Kermeen[2].

In addition to visual observations, some sound measurements were made with the ORL acoustic apparatus[5]. As with the visual observations, the velocity was held constant and the pressure was lowered until the nose cavitated all over. The static pressure was then gradually raised through the cavitation range while the hydrophone acoustic pressure readings and the working-section static pressure readings were

correlated by the observers. The result of such measurements for the 1-1/8-inch-diameter hemisphere is shown in figure 1. The shape of the curve is like that given in reference 2, figure 4, although the curve of figure 1 does not have as sharp a peak. If the maximum point is arbitrarily taken as the point of inception, we find a value of 0.64 for the incipient cavitation number at a free-stream velocity of 51 fps. This value shows good agreement with ORL visual value of 0.646 (figure 5). For the larger bodies, the difference in hydrostatic pressure from the bottom to the top of the model allows various degrees of cavitation to be distributed around the nose, from nearly incipient at the bottom, say, to more profuse cavitation at the top. This hydrostatic effect tends to make the sound peak more gradual for models which are larger than two inches in diameter. Thus, the acoustic determination loses its usefulness if the point of maximum acoustic pressure is to be used to define incipient cavitation.

For the smaller models tested at both ORL and CIT a noticeable "hysteresis"[2] in the cavitation phenomenon was observed. When the pressure was lowered rather quickly below the inception point, cavitation would not occur immediately. When cavitation finally appeared, its state was more highly developed than the incipient state of the maximum of figure 1, and it was then necessary to increase the pressure to attain incipient conditions. As mentioned previously, the general procedure of first establishing cavitation and then raising the pressure to its value for visual incipient cavitation has been found to be the most practicable for this study, as this procedure avoids the above difficulty and allows reproducible data to be obtained easily.

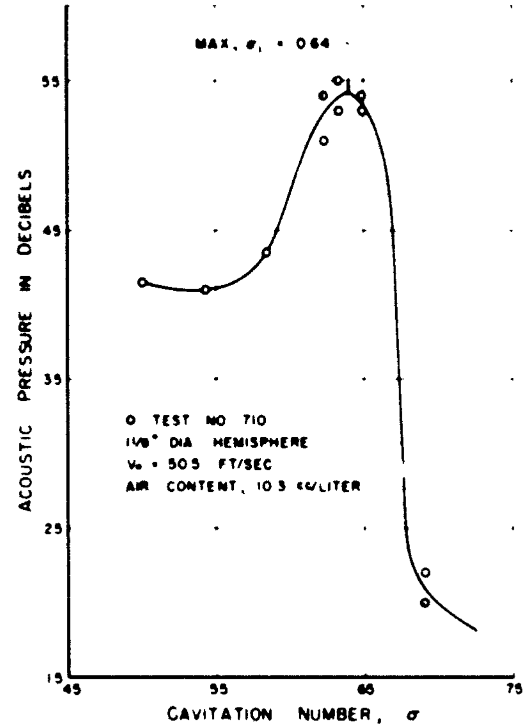

FIG. 1. NOISE GENERATED BY CAVITATION ON 1-1/8-INCH HEMISPHERE - ORL DATA

Reduction of Data

The cavitation number, σ, is a convenient parameter for describing cavitating flows. From the procedure outlined above, it is clear that p_o and V_o, which enter in the expression for σ, were not measured directly. Therefore, p_o and V_o must be obtained from the measured quantities by taking account of elementary flow laws and certain empirically derived corrections. The corrections employed here include the correction for the streamwise loss in static pressure due to the growth of the boundary layer in the working section; and for the larger models, the static pressure loss from the model centerline to the top of the model, plus a correction to the free-stream velocity to account for blockage or tunnel wall effects.* Further, all ORL data were corrected to account for the change in the velocity due to the growth of the boundary layer so that the final value of V_o represents the effective free-stream velocity along the centerline of the model.

If p_t is the measured working-section static pressure taken from taps located at the upstream end of the test section, Δp_f is the loss in static pressure due to the growth of the boundary layer along the working section between the piezometer ring and the model nose, and Δp_h is the loss in pressure from the model centerline to the top of the model, then

$$p_o = p_t - \Delta p_f - \Delta p_h^{**}$$

The mean velocity in the free stream $\overline{V}_o$ is given by

$$\overline{V}_o = k\sqrt{\Delta}$$

where Δ is the pressure differential across the nozzle and k is a constant of proportionality. For example, for the ORL tunnel, if Δ is in inches of mercury and $\overline{V}_o$ is in feet per second, k = 5.2 ft/sec (inches of Hg)$^{1/2}$.

If V_o' is the free-stream velocity in the center of the tunnel without blockage corrections, then for the ORL data

$$\overline{V}_o = 0.99 V_o'$$

while for the CIT data

$$\overline{V}_o = V_o'$$

The blockage correction factor is defined as

$$\frac{V_o^2 \text{ (without walls)}}{\left(V_o\right)^2 \text{ (with walls)}} = N \qquad \text{(c.f. Appendix B)}$$

If account is taken of all these factors, the incipient cavitation number can be written as

$$\sigma_i = \frac{p_t - \Delta p_f - \Delta p_h - p_v}{\frac{1}{2}\rho V_o^2} = \frac{1}{N}\left[\frac{p_t - p_v}{\frac{1}{2}\rho V_o^2} - C_f - C_h\right]$$

---

* Details of the blockage corrections are given in Appendix B.

** At the present time the High-Speed Water Tunnel, CIT, has an uncertainty factor within ± 2 per cent for $(p - \Delta p_f)/\frac{1}{2}\rho v_o^2$

where

$$C_f = \frac{\Delta p_f}{\frac{1}{2}\rho V_0^2}$$

and

$$C_h = \frac{\Delta p_h}{\frac{1}{2}\rho V_0^2}$$

are dimensionless coefficients for the pressure losses due to the growth of the boundary layer in the working section and the difference in elevation from the centerline to the top of the model, respectively. It has been assumed that consistent units are employed for all quantities which form the last equation so that no conversion factors need be explicitly indicated. For most of the data N=1. At ORL, blockage corrections were applied to the data on the eight-inch-diameter hemisphere only, while at CIT, blockage corrections were applied to data from both the four-inch-diameter hemisphere and the four-inch-diameter ogive. Of course, C_h is important only for the larger models or for very low velocities.

After all data had been reduced as outlined above, they were arranged in tabular forms. These tables are presented in Appendix C. Mr. R. W. Kermeen has kindly permitted the authors to use those portions of his experimental data which apply to the present study. Since he has given no tables of data in reference 2, we have included these data with our own test results in Appendix C.

Discussion of Results

Dependence of σ_i on V_o

The CIT and ORL data are presented in figures 2 through 12, where the incipient cavitation number for each model size is shown as a function of the free-stream velocity. The average air content for each model is also shown in the figures. The eight-inch-diameter hemisphere was not tested at CIT.

Except for the one-fourth-inch hemisphere (figure 2), the CIT data shown in figures 2 through 12 are generally slightly higher than the ORL data. In most cases, this difference appears to be well within the experimental error one would expect in the two test facilities. In addition to dissimilarities in instrumentation and control, a resorber[4] is employed in the circuit of the High-Speed Water Tunnel to redissolve entrained air, whereas the ORL tunnel is not equipped for this. In view of these differences in the facilities and those in the test procedure, the over-all agreement of the test results is very satisfactory.

Curves were faired through the data of figures 3 through 12 and the accumulative results are given in figure 13. Because of the wide spread in the data for the one-fourth-inch hemisphere, no attempt was made to obtain a faired curve. Except for the smaller hemispheres at low velocities, figure 13 shows that the incipient cavitation number increases with both velocity and size. The cross plot of figure 13 excluding the low velocity range is shown in figure 14.

It is customary to assume that $\sigma_i = |C_{p_{min}}|$ on the body, and hence for comparison purposes, the absolute value of the minimum pressure coefficient is shown in figure 13 for both the hemispheres and ogives. These values of the minimum pressure coefficient are for Reynolds number in the supercritical range[6]. Except for the eight-inch hemisphere, all values of σ_i are below $|C_{p_{min}}|$. This shows that the conventional method of calculating the incipient cavitation index is not valid.

It was observed both at ORL and at CIT that wide variations in the dissolved air content made no systematic differences in the test results (except in the case of the one-fourth-inch hemisphere at very low velocities). The nondependence of the incipient cavitation number upon air content is typified by the CIT data plotted in figure 10 for the one-inch-diameter 1.5-caliber ogive.

The data obtained from the tests on the one-fourth-inch hemisphere are shown in figure 2. In particular, the CIT data become more scattered as the velocity, V_o, decreases, and the data taken at the higher air content tend to lie above the data for the lower air content. Also, these data show a reversal of the general trend exhibited by figures 5 through 12 in that for the low velocity range, σ_i increases with a decrease in the velocity. This trend is also shown by the CIT data for the three-eighths-inch and one-half-inch hemispheres in figures 3 and 4. In contrast to the data for the smaller hemispheres, the ogive data do not show a reversal of the general trend in the low velocity range. However, the ogive data do not extend far enough into the low velocity range to justify definitely concluding that a reversal of the general trend does not exist. Kermeen[2] found that by employing a special test procedure, clear cavities up to 23 model diameters in length could be established on small hemispheres at very low velocities. In some cases, the cavities were maintained at cavitation numbers as high as 4.8. This phenomenon, which was apparently due to air diffusion, may account for the reversal of the general trend shown by

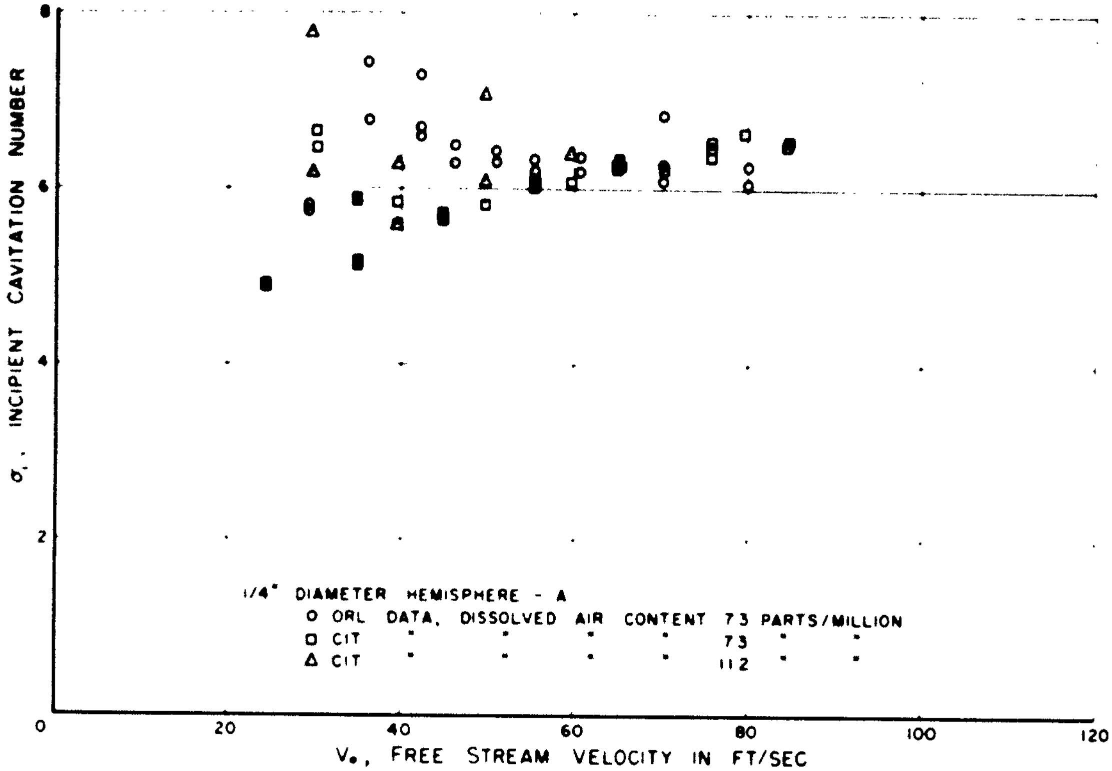

[illegible] NUMBER VS FREE STREAM VELOCITY
[illegible] HEMISPHERE [illegible] AND ORL DATA

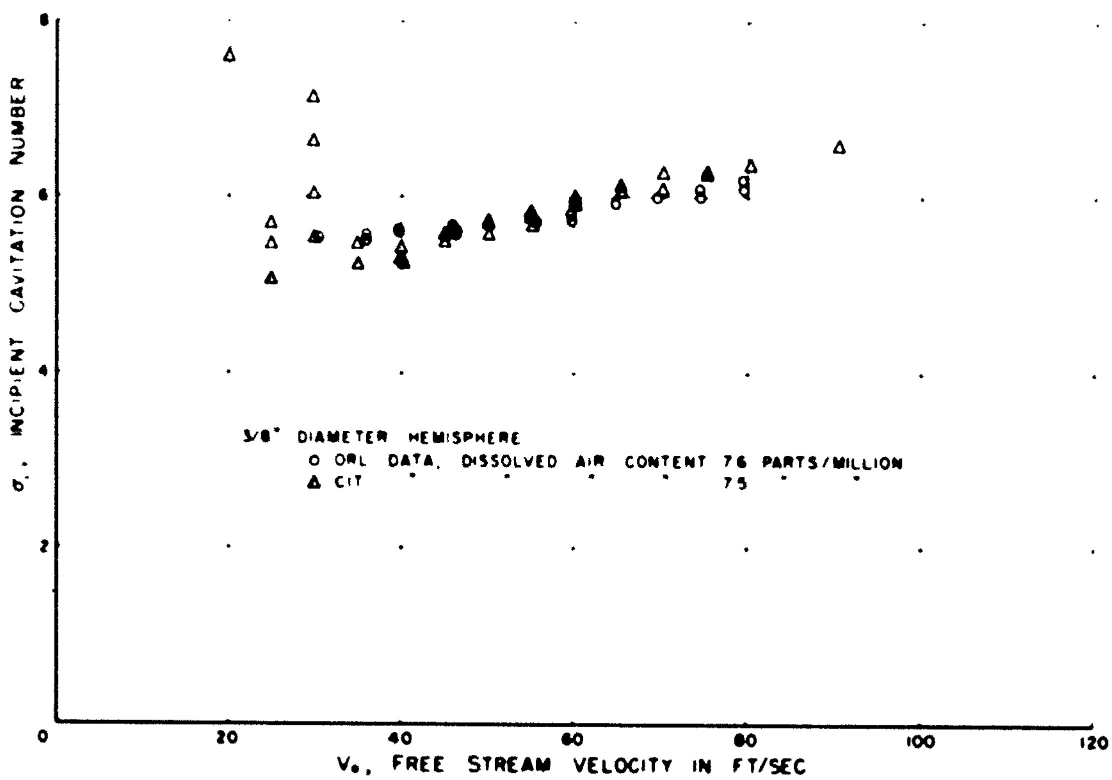

[illegible] FREE STREAM VELOCITY
[illegible] HEMISPHERE [illegible] DATA

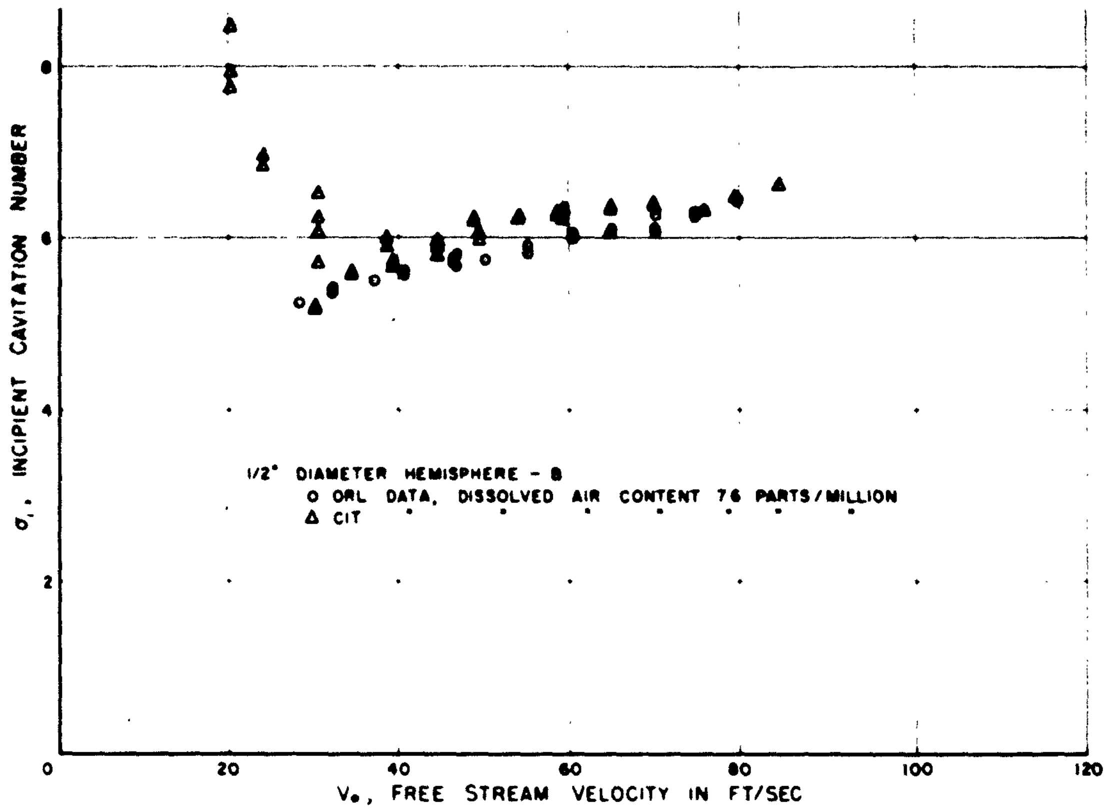

FIG. 4 INCIPIENT CAVITATION NUMBER VS FREE-STREAM VELOCITY
FOR 1/2-INCH HEMISPHERE - CIT AND ORL DATA

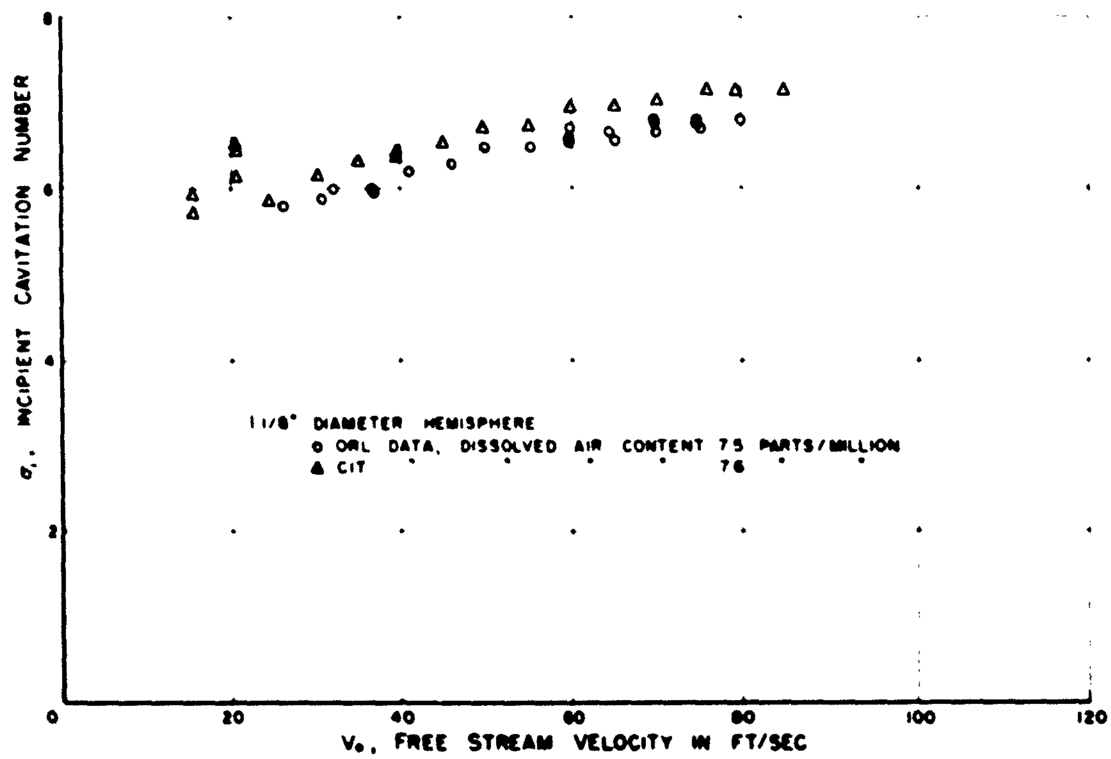

FIG. 5 INCIPIENT CAVITATION NUMBER VS FREE-STREAM VELOCITY
FOR 1-1/8-INCH HEMISPHERE - CIT AND ORL DATA

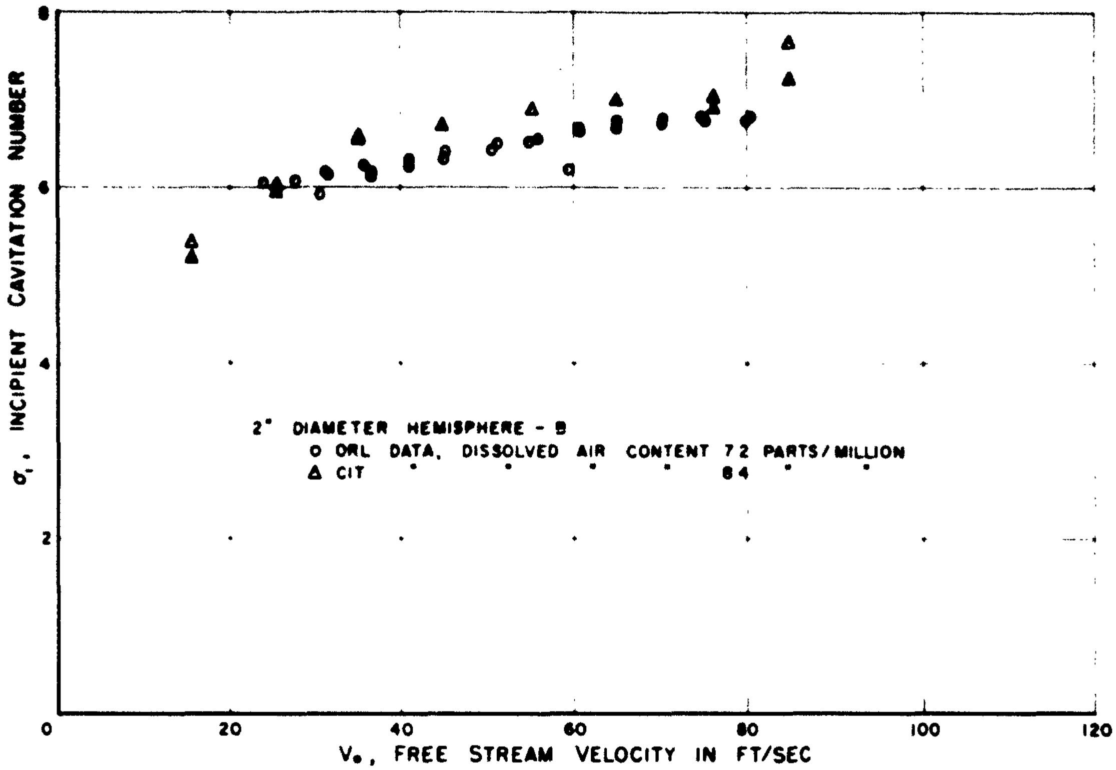

FIG. 6 INCIPIENT CAVITATION NUMBER VS FREE-STREAM VELOCITY FOR 2-INCH HEMISPHERE - CIT AND ORL DATA

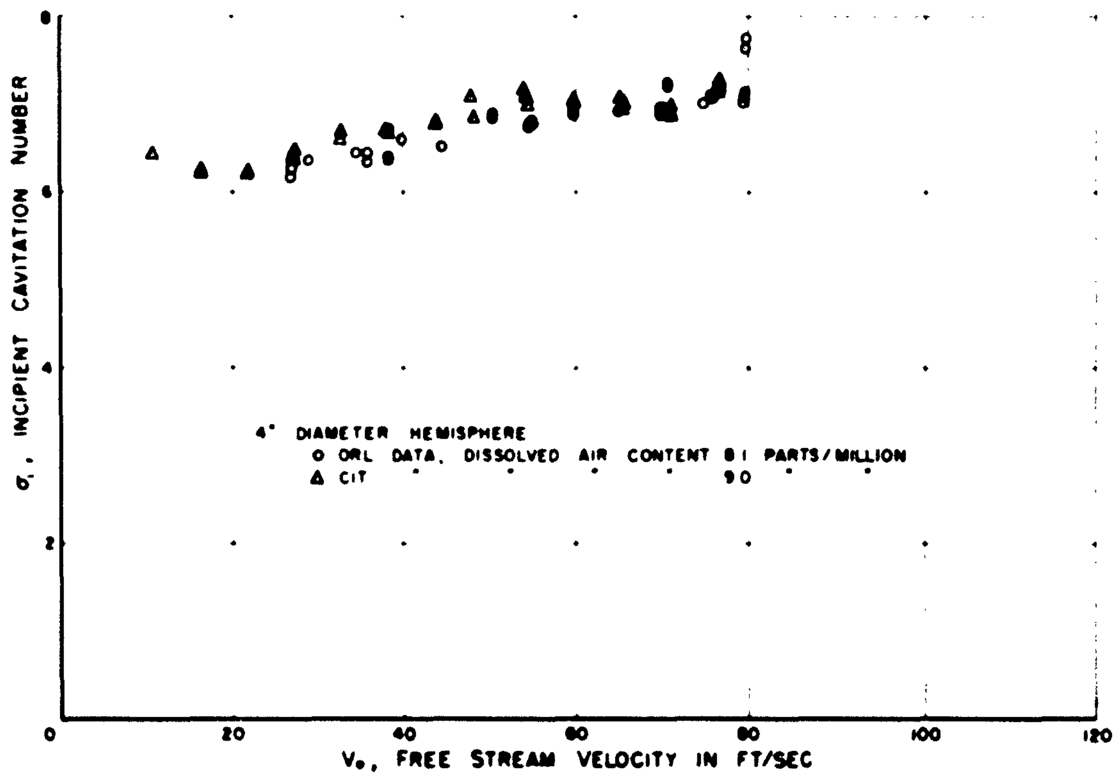

FIG. 7 INCIPIENT CAVITATION NUMBER VS FREE-STREAM VELOCITY FOR 4-INCH HEMISPHERE - CIT AND ORL DATA

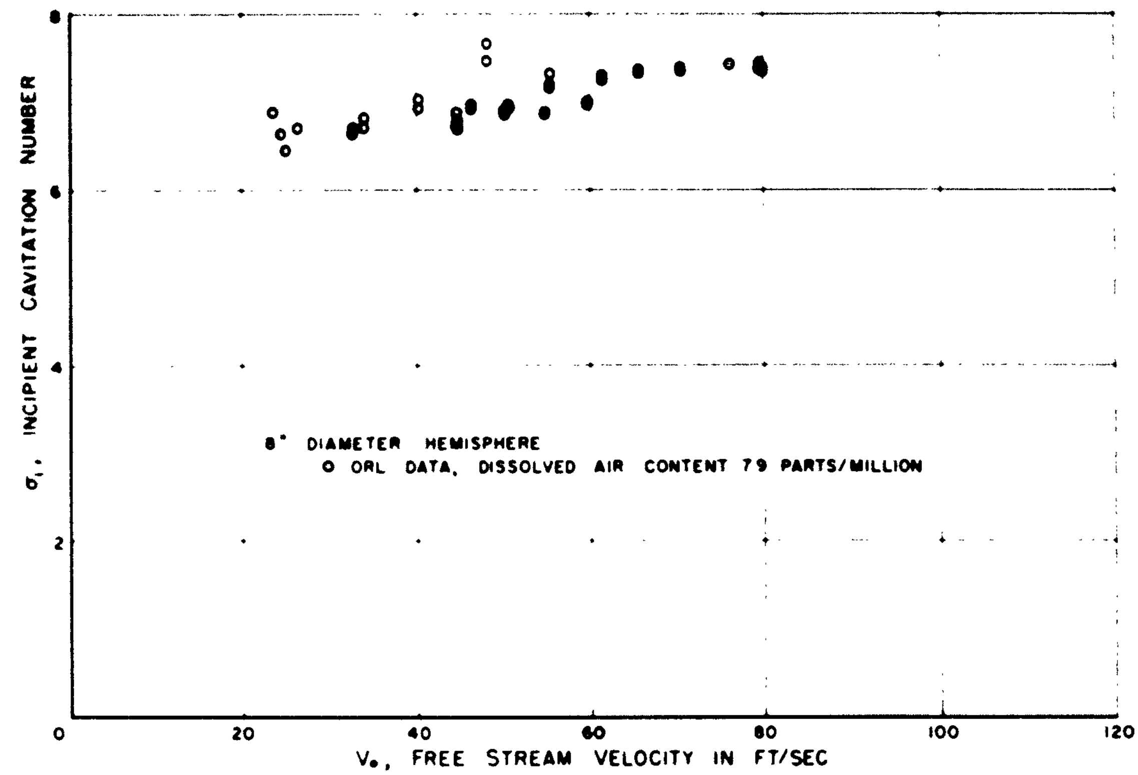

FIG. [illegible] INCIPIENT CAVITATION NUMBER VS FREE-STREAM VELOCITY
FOR 8-INCH HEMISPHERE - ORL DATA

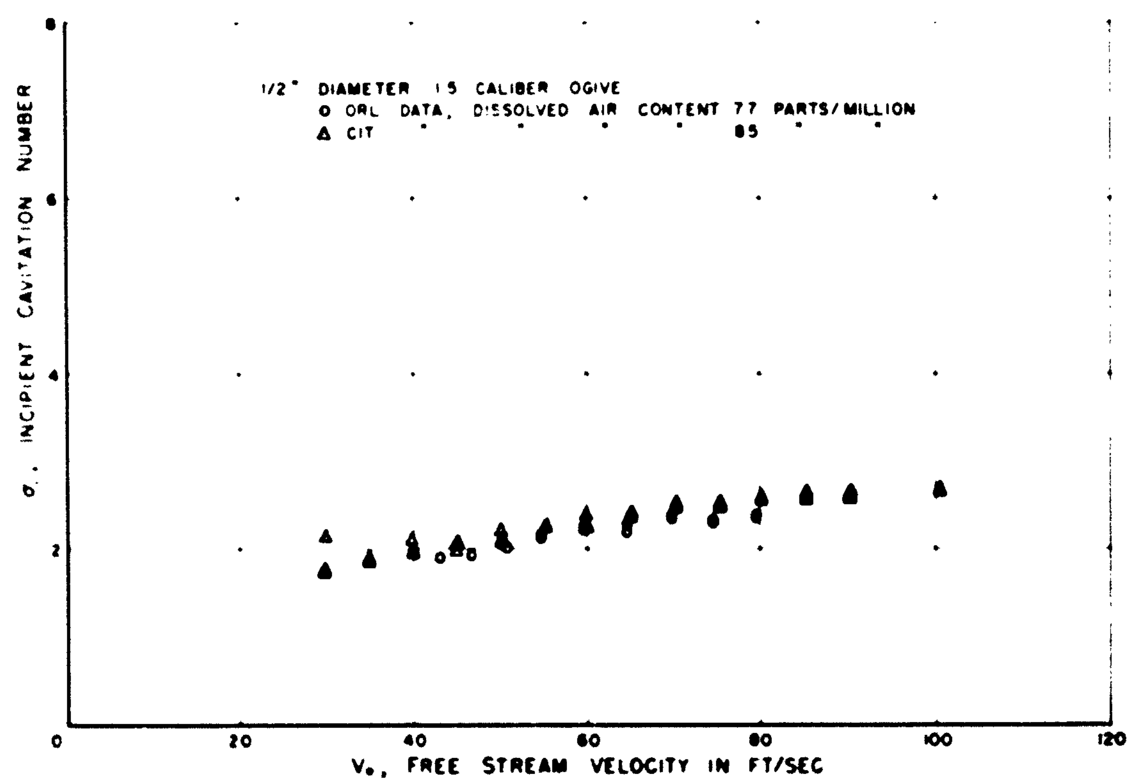

FIG. [illegible] INCIPIENT CAVITATION NUMBER VS FREE-STREAM VELOCITY
FOR 1/2-INCH OGIVE - CIT AND ORL DATA

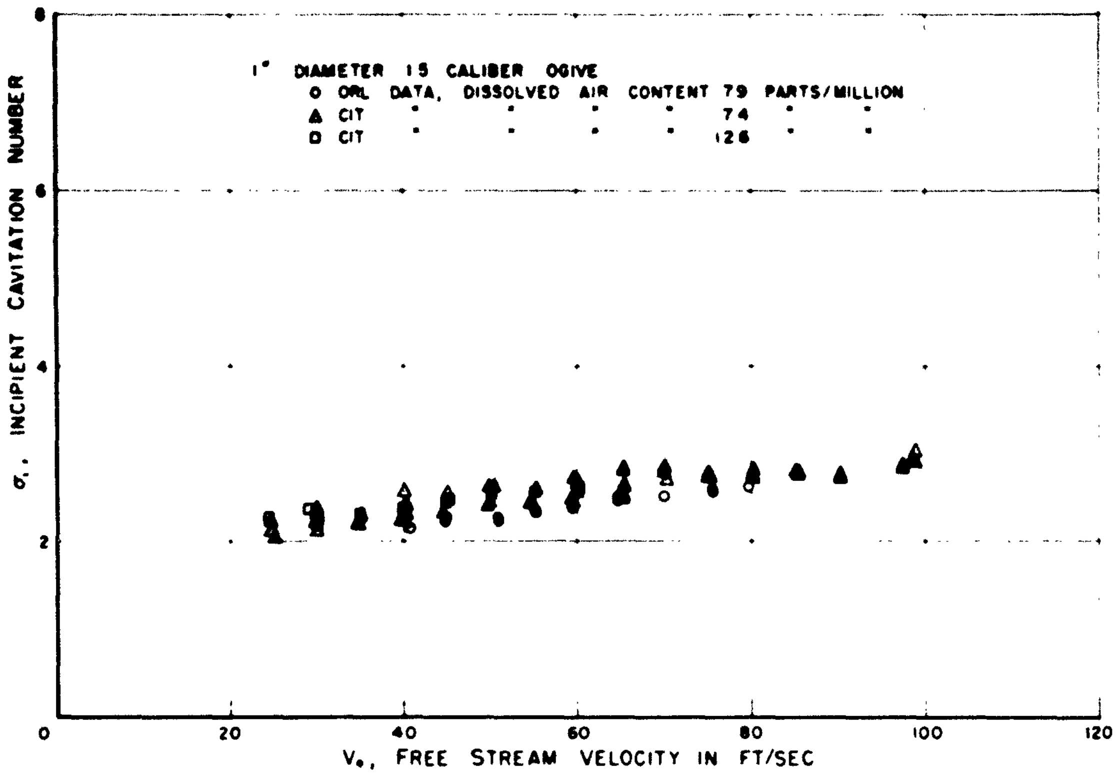

FIG. 10. INCIPIENT CAVITATION NUMBER VS FREE-STREAM VELOCITY FOR 1-INCH OGIVE - CIT AND ORL DATA

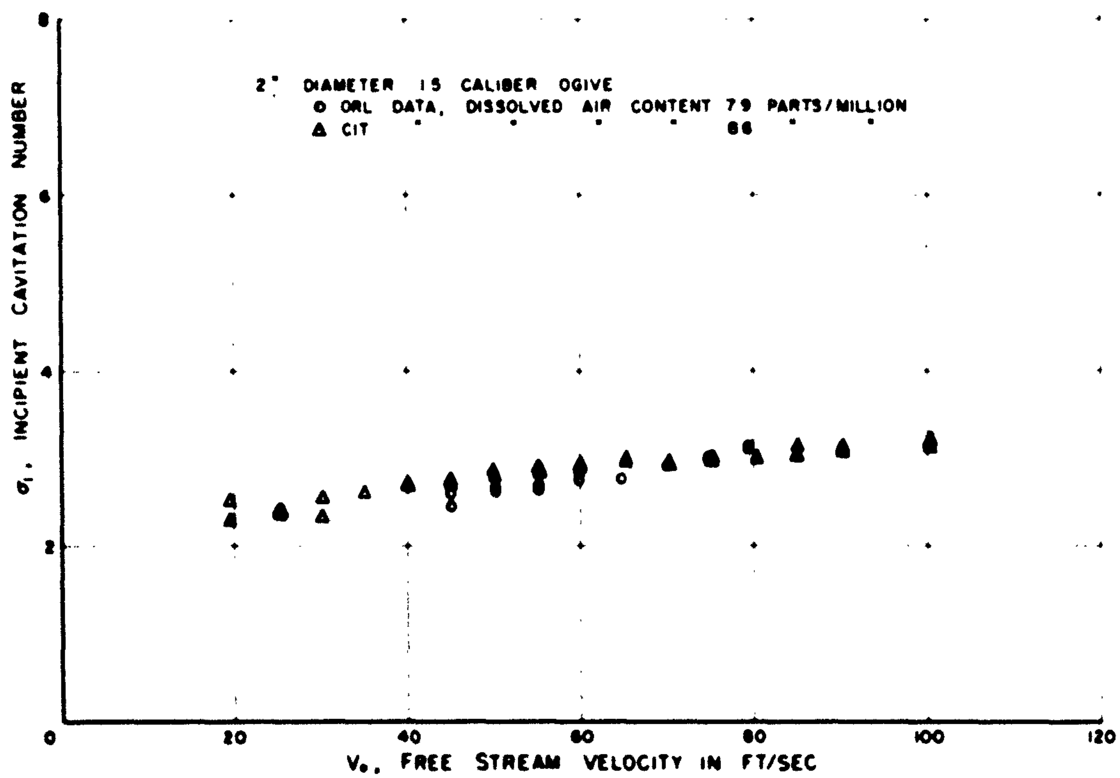

FIG. 11. INCIPIENT CAVITATION NUMBER VS FREE-STREAM VELOCITY FOR 2-INCH OGIVE - CIT AND ORL DATA

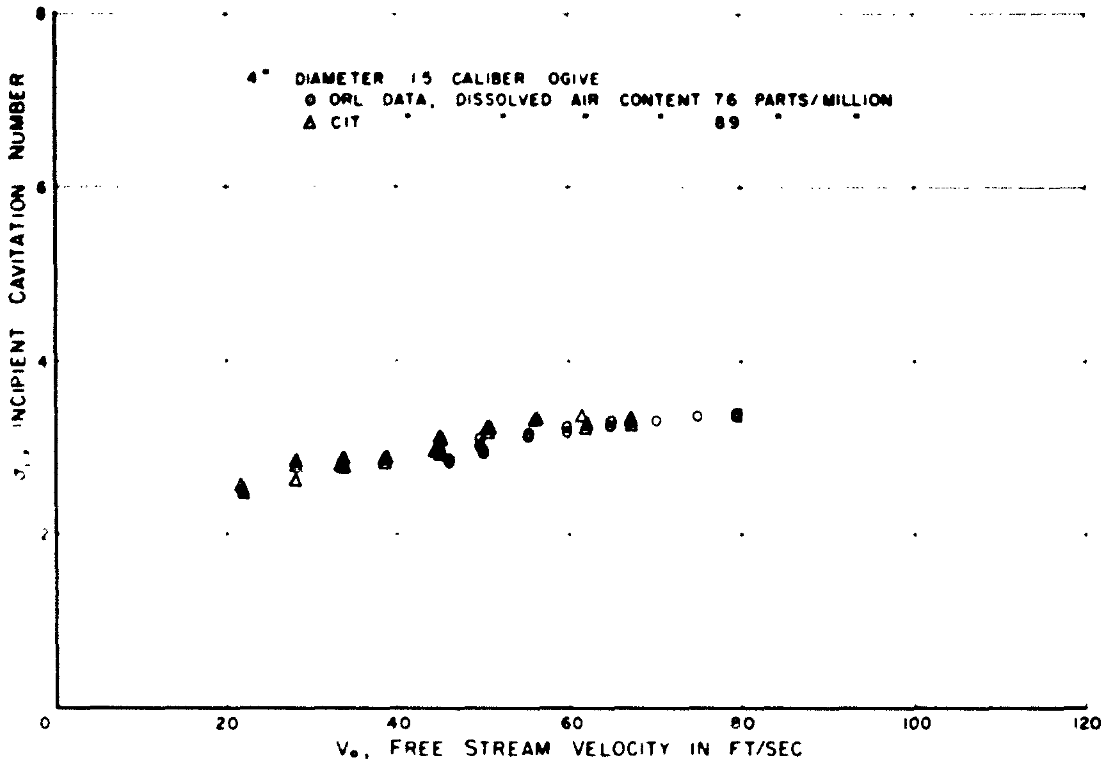

[illegible] FREE STREAM VELOCITY
[illegible] DATA

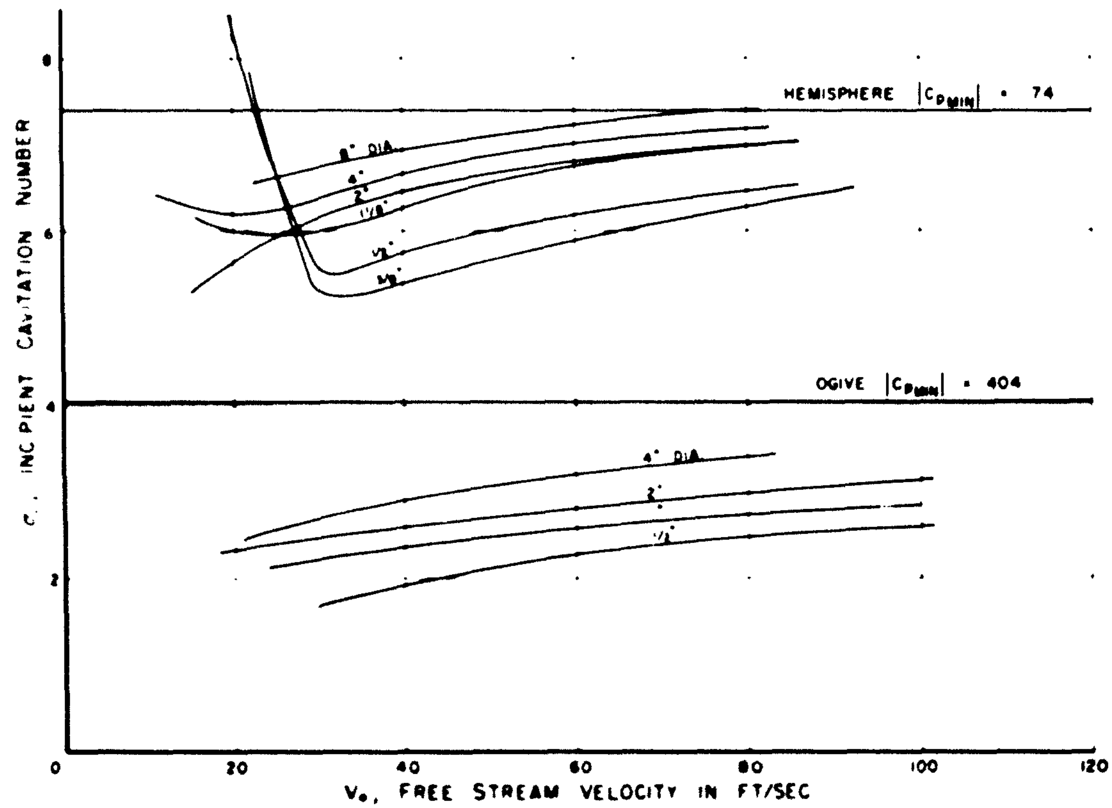

[illegible] FREE-STREAM [illegible]
[illegible] HEMISPHERE AND OGIVE MODELS

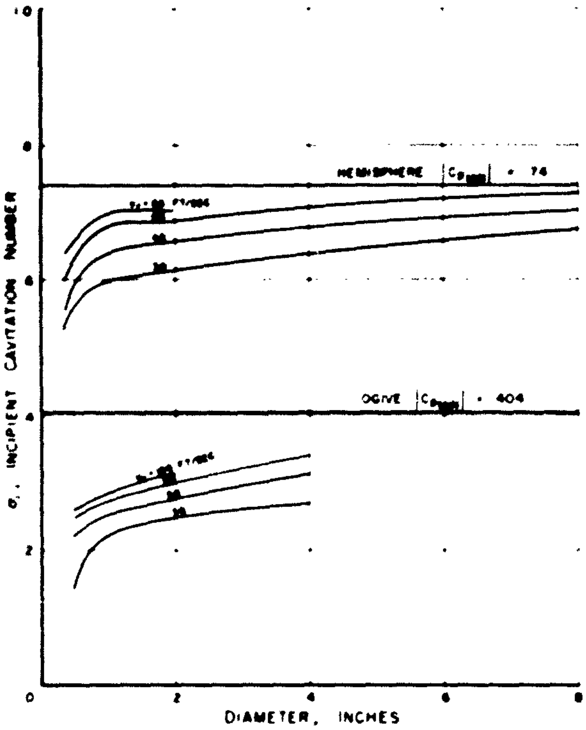

FIG. 14 EFFECT OF MODEL SIZE UPON INCIPIENT CAVITATION FOR SEVERAL VALUES OF THE FREE-STREAM VELOCITY

the one-fourth-inch, three-eighths-inch, and one-half-inch hemispheres.

Part of the scatter shown by the ORL data for the one-fourth-inch hemisphere may be due to difficult conditions of observation in the 48-inch tunnel. In order to see cavitation on the model in the test section, it was necessary to look through some two feet of water. In addition, the reflection of intense highlights from the shiny surface of the model hindered visual observation, so that incipient cavitation was difficult to define. However, the ORL data for the one-fourth-inch nose have less scatter than the corresponding CIT data. But at CIT, since the test section is much smaller, visual observations were not difficult. Hence, we may conclude that the trend so clearly shown by the data represents an actual difference in the nature of incipient cavitation when the model size and free-stream velocity are sufficiently reduced.

The spread in the data for the eight-inch hemisphere was due to surface roughness and entrained air. Small diamond-shaped cavitation zones apparently due to very small rough spots became fixed at random points on the nose for a long time before they were swept away. In some cases these points of apparent roughness seemed to shift to another spot. These diamond-shaped cavitation patches were also characteristic of the four-inch hemisphere; however, they were less severe than those for the eight-inch hemisphere. Recent tests of a two-inch-diameter hemisphere having a somewhat rough finish showed that similar diamond-shaped patches appeared at high velocities. Possibly this is due to the boundary layer becoming thinner as the velocity is increased, with the resulting protrusion of large roughnesses causing cavitation. Polishing the eight-inch hemisphere appeared to help somewhat, but did not completely remove the small diamond-shaped cavitation zones. When such zones were near the top of the model, the observation of inception conditions was difficult. Further, at low pressures the cavitation zone around the eight-inch model was confused by growing air bubbles and entrained air, so that observations of the inception of cavitation were made more uncertain. This type of air-bubble growth was observed to be more pronounced as the nose size was increased, probably because the larger the model the greater the time available for the air bubbles to grow at any given free-stream velocity. The situation was improved by raising the pressure to 40 psia for ten minutes (as mentioned under Test Procedure, page 2) to drive the entrained air back into solution. Then the pressure was lowered and readings were taken before air came out of solution. We believe that the greater scatter shown by the test results for the eight-inch model (figure 8) is largely due to the above effects.

Dependence of σ_i on Reynolds Number

The ORL and CIT data for incipient cavitation number are shown as a function of Reynolds number in figures 15 and 16, respectively. Referring to figure 15, the ORL data indicate that the incipient cavitation number is not a unique function of Reynolds number, for a distinct curve could be drawn for each model size. This trend is also shown by the CIT data in figure 16. Although there may be some Reynolds-number effects, we do not yet understand their full significance. We believe that such effects could influence the bubble growth required to produce incipient cavitation by their influence upon the time available for the occurrence of such growth[3].

Dependence of σ_i on $Vd^{1/2}$

On the basis of a dimensional analysis, J. W. Holl concluded that it might be useful to express the incipient cavitation number as a function of the Weber number based upon the model diameter. Thus, if s is the surface tension of the water, V_0 is the free-stream velocity, ρ is

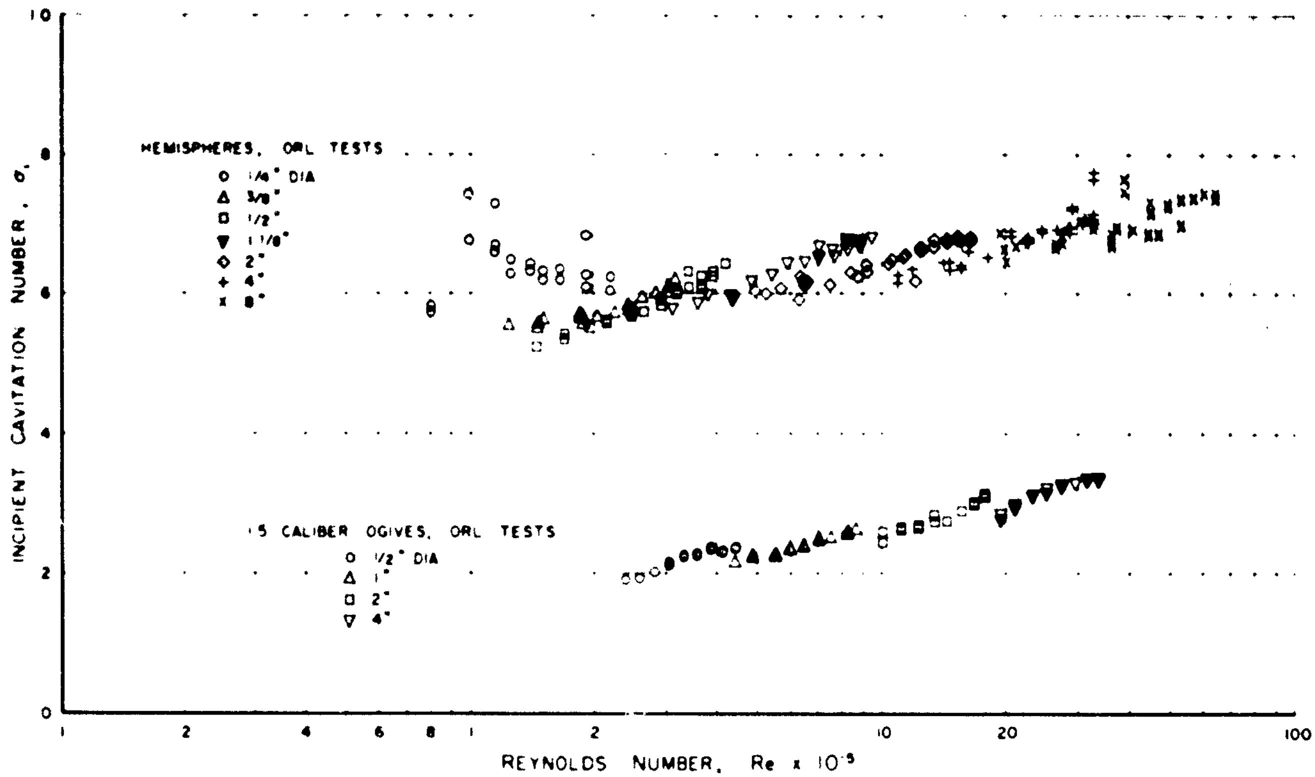

FIG. 15. INCIPIENT CAVITATION NUMBER VS REYNOLDS NUMBER—ORL DATA

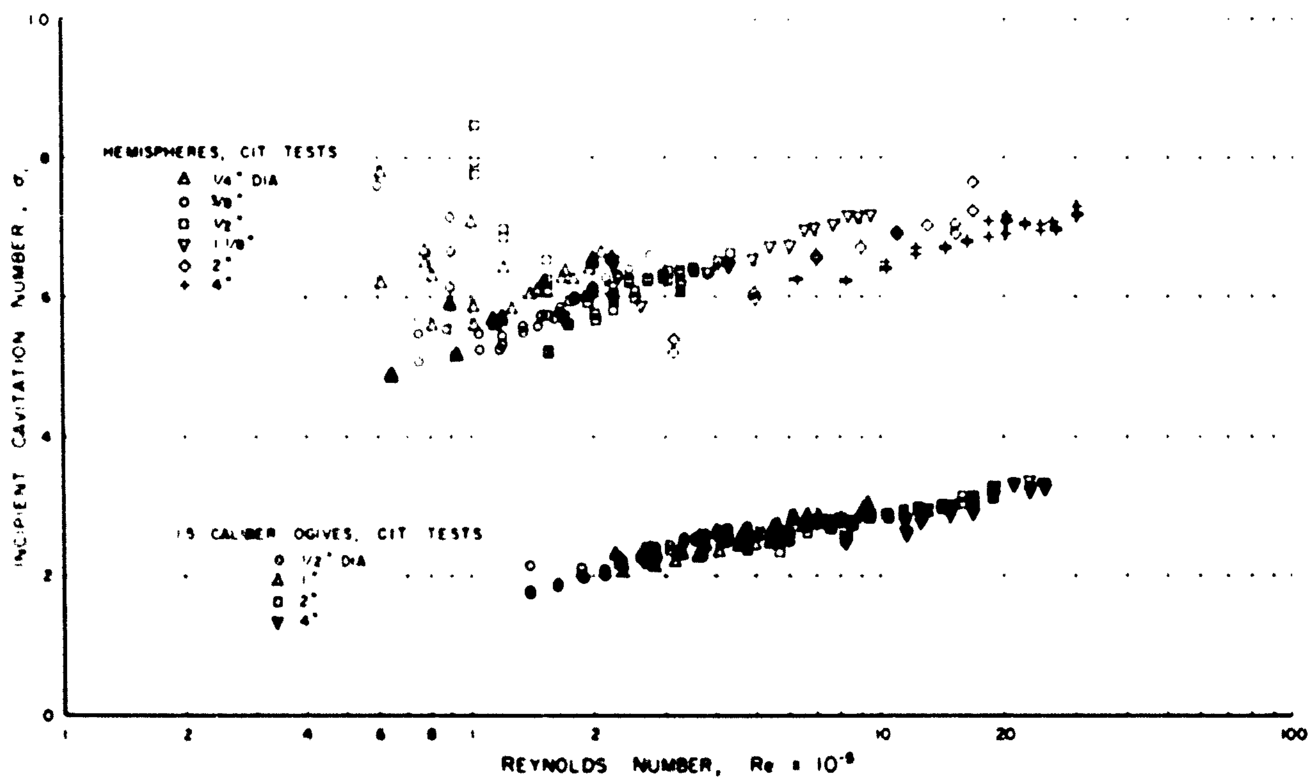

FIG. 16. INCIPIENT CAVITATION NUMBER VS REYNOLDS NUMBER—CIT DATA

the liquid density and d is the maximum diameter of the body, the Weber number of interest here is given by

$$W_e = \frac{V_0\sqrt{d}}{\sqrt{s/\rho}}$$

However, the correlation of the experimental data for σ_i with W_e would imply a more general result than can actually be inferred from these Water Tunnel tests, because the ratio s/ρ was not significantly altered during these experiments.

For example, table I below shows only a 3.38-percent variation in s/ρ when the water temperature is changed from 70 to 100 degrees F. Actually the temperature variation encountered in the course of the present experiments was somewhat less than 70 to 100 degrees F, so that the variation in the ratio, s/ρ, was less than 3.38 per cent. Such a variation is not of engineering significance.

The ORL data for incipient cavitation number were plotted as a function of Weber number, and the results showed that σ_i could be represented by a single curve for each model shape. However, as shown previously, the ratio s/ρ was not varied significantly, so that one could only conclude that σ_i was a function of $V\sqrt{d}$. The ORL and CIT data were then plotted as a function of $V\sqrt{d}$, and the results are shown in figures 17 through 20. The hemisphere data obtained at ORL and CIT are shown in figures 17 and 18, respectively. Although there is some scatter in the data, we see that, for the most part, there are no consistent variations in the data because of changes in model size. The ORL and CIT data for the 1.5-caliber ogives given in figures 19 and 20 show the same correlation as did the hemisphere data, but in this case, there is less scatter** in the data. Thus it appears possible to represent the data by a single curve for each of the four figures. For comparison purposes, a curve was faired through the experimental points for each of figures 17 through 20, and from these faired curves figure 21 was constructed. The over-all trends for the ogive and hemisphere experiments are very much alike for both laboratories. The more detailed differences in the curves of figure 21 appear to be within the experimental scatter of the plots in figures 17 through 20.

Table I - Values of s/ρ as a Function of Water Temperature*

Water Temperature (degrees F)	s/ρ (ft^3/sec^2)
50	0.002619
60	0.002595
70	0.002564
80	0.002544
90	0.002518
100	0.002485
120	0.002430

* Values of s were taken from reference 7.

From the foregoing it is clear that the present experiments indicate a correlation between the incipient cavitation number σ_i and the parameter $V_0\sqrt{d}$. We regret that the ratio of surface tension to density, s/ρ, could not also be varied so that the dependence of σ_i upon Weber number could be investigated. We believe that it may be profitable to perform similar cavitation studies in different liquids to investigate the Weber-number dependence.

** Deviations from the theoretical body shape would not be so critical in the case of the ogives because of the flatter pressure distribution; hence, this would probably account for the smaller amount of scatter in the data.

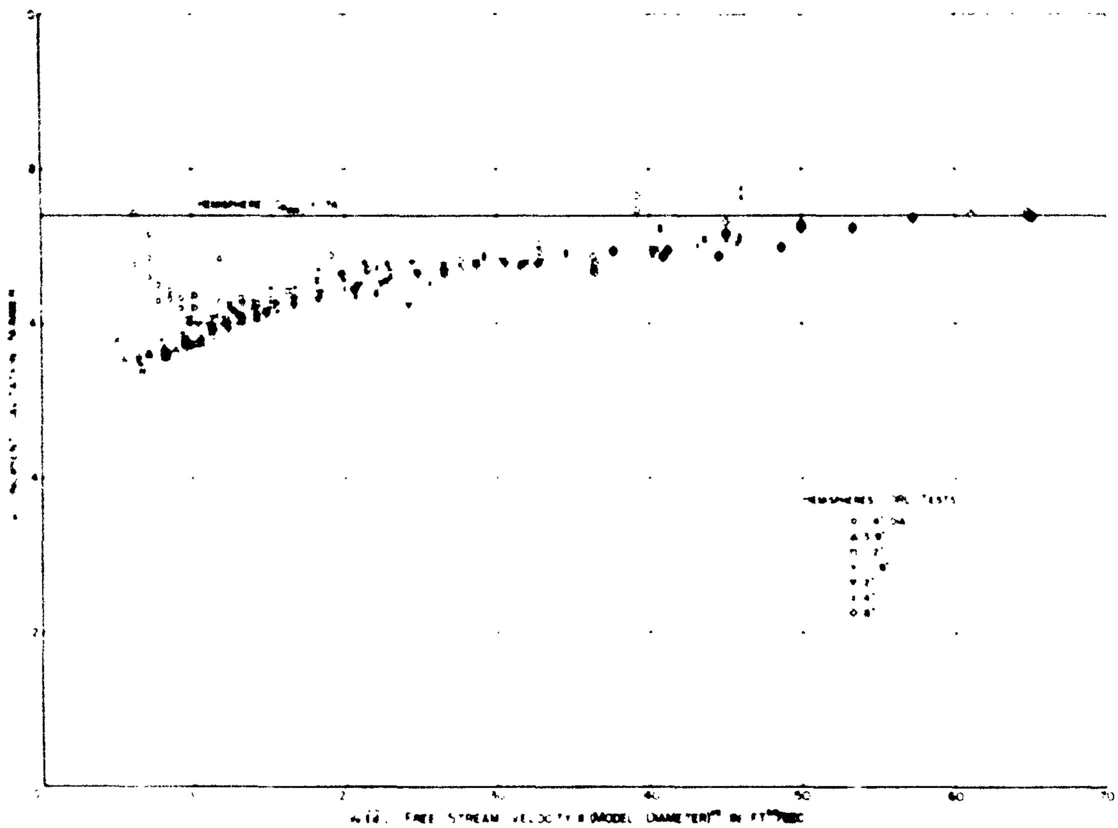

FIG. 17. CORRELATION OF ORL HEMISPHERE DATA WITH $V_0\sqrt{d}$

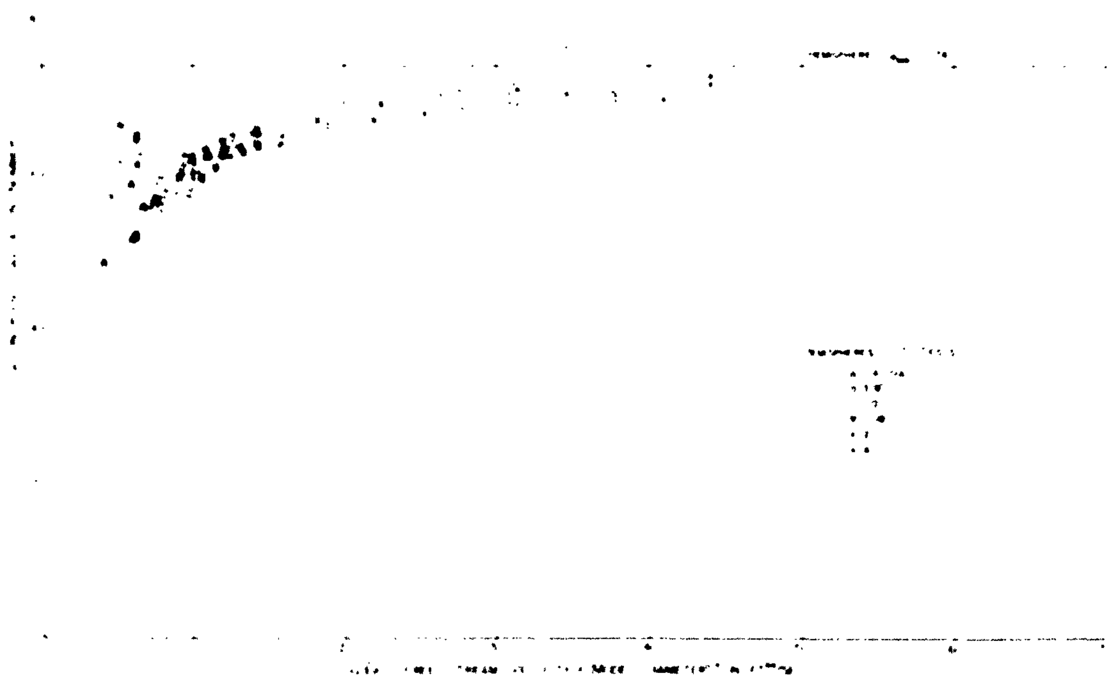

FIG. 18 CORRELATION OF CIT HEMISPHERE DATA WITH $V_0\sqrt{d}$

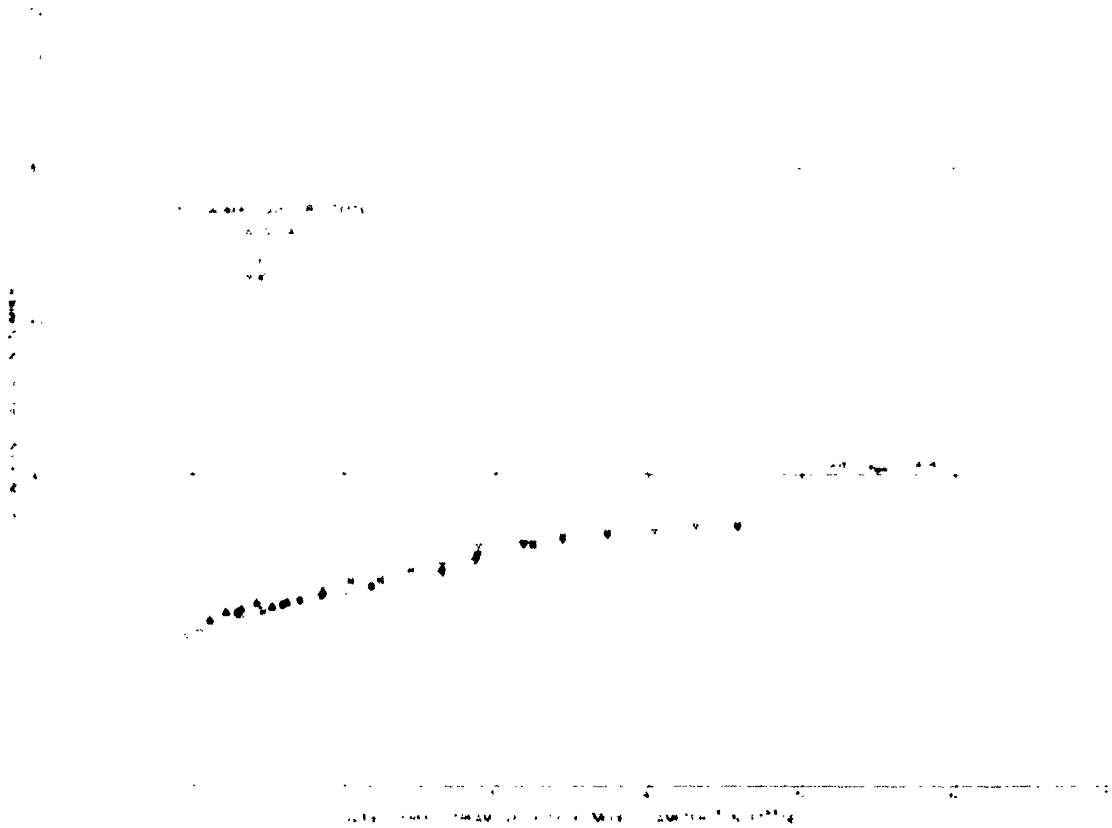

FIG. 19 CORRELATION OF ORL OGIVE DATA WITH $V_o\sqrt{d}$

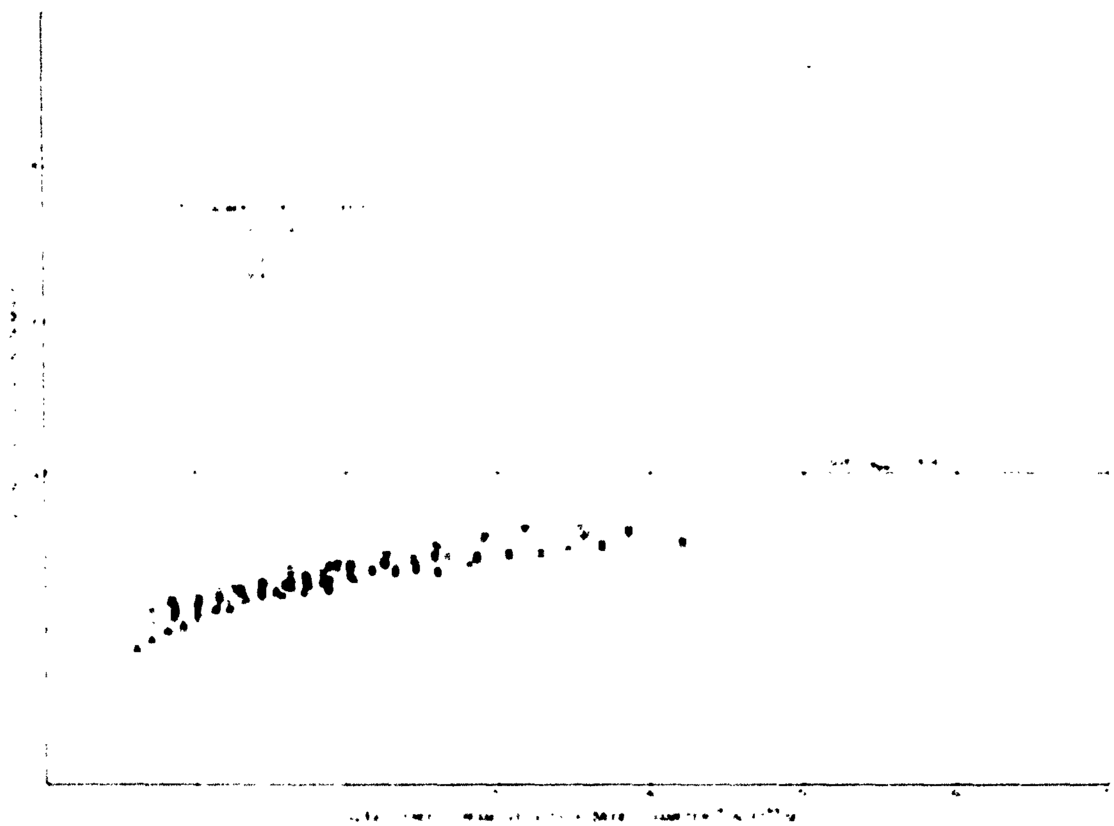

FIG. [illegible] CORRELATION OF [illegible] OGIVE DATA WITH $V_o\sqrt{d}$

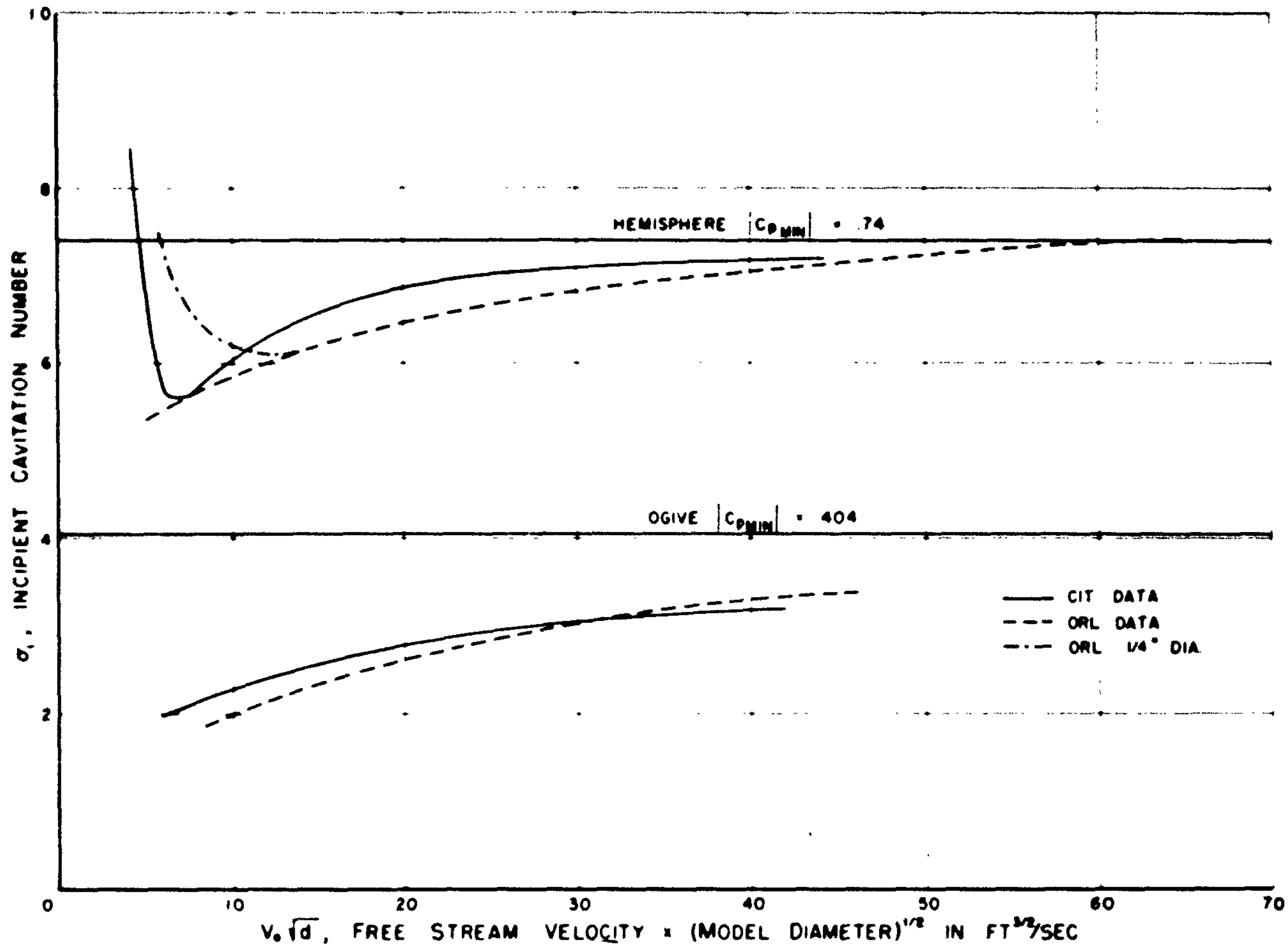

FIG. 21. A COMPARISON OF $V_0\sqrt{d}$ CORRELATIONS OBTAINED AT CIT AND ORL

Conclusions

The ORL experiments verify the CIT findings which show that the inception of cavitation in a steady rectilinear flow of a liquid past a body depends upon the free-stream velocity and the body size. This result was found to hold for hemisphere-nosed bodies up to eight inches in diameter, while the largest bodies tested before were two inches in diameter. In general, it was verified that the incipient cavitation number increases with body scale and free-stream velocity. Except for the largest body at higher flow velocities, the measured values of the incipient cavitation number are not as great as the incipient cavitation number which would be found by the customary calculation procedure. Hence, at the inception point, the pressure external to the cavities is not in general equal to the vapor pressure as is so often assumed. However, for full-scale work, it is safe to assume that $\sigma_i \cong |C_{p_{min}}|$.

Except for the smaller hemispheres at the lower velocities (less than 30 fps) no consistent variations of the incipient cavitation number with air content were observed.

The results for the smaller hemispheres at lower velocities showed a tendency for the incipient cavitation number to increase with increasing dissolved air content. Also, in the low velocity range, the incipient cavitation number increased with a decrease in the velocity. This phenomenon was a reversal of the general trend characteristic of the larger hemispheres and all of the 1.5-caliber ogives. Evidently, this exceptional behavior is caused by air diffusion from the liquid into the cavitation bubbles. Data having sizable scatter and poor reproducibility are characteristic of tests made on small models at low velocities; consequently, these test conditions should be avoided when the results of model tests are used for predicting the performance of larger scale bodies.

It has been found possible to represent the data from the present experiments as a function of the parameter $V_0\sqrt{d}$ for each family of shapes tested. Of course, the data are also representable in terms of the Weber number, $V_0\sqrt{d}/\sqrt{S/\rho}$, because the ratio of surface tension to density, S/ρ, was not significantly varied in these experiments. Further experiments with other liquids should be undertaken to see if the more general correlation of the incipient cavitation number with Weber number is meaningful.

Appendix A

Models and Test Configurations

Seven hemispherical heads and four 1.5-caliber ogive heads were used in these experiments. The pertinent details concerning these head forms are given in table A-1. The designations A and B for the two-inch, one-half-inch, and one-fourth-inch hemispheres correspond to those used in references 1 and 2. The Ordnance Research Laboratory has two four-inch hemispheres designated A and B, and as shown in table A-1, nose B was used in these studies. The eight-inch hemisphere was not tested at CIT.

At ORL the one-fourth-inch to two-inch noses were supported in the Tunnel on a two-inch cylindrical brass body with a conical tail. The four-inch and eight-inch noses were supported on a four-inch cylindrical brass body with a conical tail and with a wooden fairing to fair the eight-inch nose into the four-inch supporting body. These bodies were supported from the Tunnel floor by a thin aluminum strut so that the axis of the models coincided with the centerline of the Tunnel test section. A pictorial description of the mounting arrangements of the various noses is given in table A-2. In this table, "L" refers to the straight section behind the nose, which was measured from the point where the nose joins the straight section. The B arrangement is typified by the four-inch hemisphere with its supporting structure, shown in figure A-1.

At CIT the test arrangement for the one-half-inch, one-inch, and two-inch ogives was

FIG. A-1 ORL ARRANGEMENT FOR SUPPORTING 4-INCH HEMISPHERE

Table A-1 Hemispheres and Ogives

Diameter (inches)	Type	Material	Made by	Maximum Deviation from Theoretical Shape
8	Hemisphere	Brass	ORL	Not inspected
4 (B)	"	Brass	ORL	Not inspected
2 (B)	"	Stainless Steel	CIT	Not given in Ref. 2
1 1/8	"	Stainless Steel	CIT	"
1/2 (B)	"	Stainless Steel	CIT	"
3/8	"	Stainless Steel	CIT	"
1/4 (A)	"	Stainless Steel	CIT	0.0003" (Ref. 2)
4 (1.5 caliber)	Ogive	Brass	ORL	Not inspected
2 (1.5 caliber)	"	Stainless Steel	CIT	0.0020"
1 (1.5 caliber)	"	Stainless Steel	CIT	0.0020"
1/2 (1.5 caliber)	"	Stainless Steel	CIT	0.0010"

Table A-2 - Mounting Arrangements

O.R.L. Experiments

Nose Size and Type	Arrange-ment	L/D
1/4" Hemisphere	A	8
3/8" "	A	8
1/2" "	A	8
1 1/8" "	A	3
2" "	B	5.5
4" "	B	4.5
8" "	C	1.5
1/2" Ogive	A	4
1" "	A	1.5
2" "	B	5.5
4" "	B	4.5

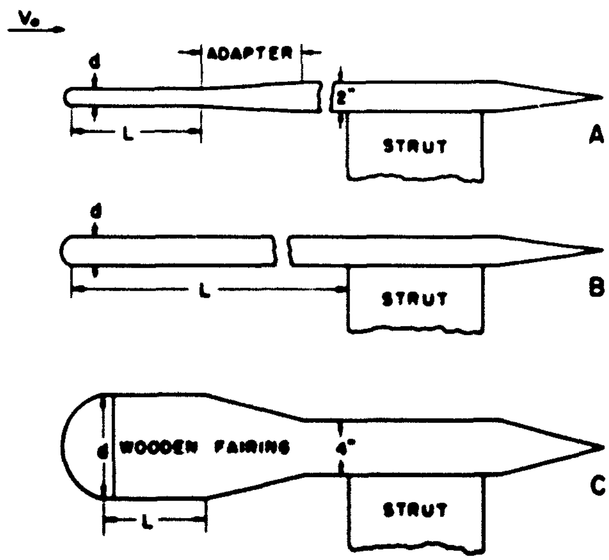

FIG. A-2 THE 4-INCH 1.5-CALIBER OGIVE MODEL INSTALLED IN THE HIGH-SPEED WATER TUNNEL

equivalent to the arrangements used at ORL. The models were supported from the bottom of the High-Speed Water Tunnel test section. The data for the one-fourth-inch to two-inch hemispheres were taken by R. W. Kermeen. A sting support was used for all models in his experiments. The details of his setup are given in reference 2. The CIT cavitation tests for the four-inch hemisphere and ogive were made on models which were supported as shown in figure A-2. This method of support was also used for the pressure distribution tests which were run to determine wall-effect correction factors (Appendix B).

Appendix B

Corrections for Tunnel Constraint

The elementary ideas behind the tunnel blockage corrections are described in Appendix A of reference 1. It was found that the blockage correction factor, N, could be defined by

$$N = \frac{C'_{p_{min}}}{C_{p_{min}}} = \left(\frac{V_0}{V'_0}\right)^2$$

where V_0 and $C_{p_{min}}$ are the free-stream velocity and minimum pressure coefficient, repectively, for unconstrained flow. The quantities V'_0 and $C'_{p_{min}}$ are the corresponding free-stream velocity and minimum pressure coefficient as measured in the water tunnel where the flow is constrained. The blockage correction factor, N, is defined so that for equal free-stream static pressures, the minimum static pressure is the same for both flows. For incipient cavitation, it follows that

$$\sigma_i = \frac{\sigma'_i}{N}$$

where σ_i is the incipient cavitation number for the constrained water-tunnel flow and σ_i is the incipient cavitation number in the equivalent unconstrained flow.

When a systematic series of pressure distributions for various degrees of blockage on a given shape is available, the blockage factor N is easily determined. Such experimental pressure distributions have been reported by the Iowa Institute of Hydraulic Research[8] for a family of hemispheres. The correction factors derived from the Iowa tests are plotted against the model diameter to working section diameter ratio, d/D, in figure B-1.

Pressure distribution tests for a four-inch-diameter hemisphere were made at CIT to check the Iowa results. The averaged and faired results of these tests are shown in figure B-2. The blockage correction factor, N, calculated from the minimum C_p of figure B-2 is shown by the square symbol in figure B-1.

The incipient-cavitation data for the four-inch-diameter hemisphere taken at CIT was corrected for blockage by using both the Iowa and CIT correction factors. A comparison of the corrected CIT data with the ORL data for the four-inch hemisphere is shown in figure B-3. One can see that the CIT data corrected by the Iowa correction factor agree more closely with the ORL results, which needed no correction. Consequently, the CIT data for the four-inch hemisphere presented in this report were corrected by the Iowa blockage factor.

Blockage data were not available for the ogive noses, so a series of pressure distribution experiments was made at CIT. The average pressure distributions for 1.5-caliber ogive noses of two-inch, three-inch and four-inch diameter are shown in figure B-4. The C_p curve for the two-inch model corresponds to unconstrained flow, and the minimum C_p obtained from the curve is -0.398, while a similar Iowa result[6], obtained by interpolation, gives -0.410 for the minimum C_p. For computing N, a value of -0.404 was taken for the minimum C_p in unconstrained flow. The resulting blockage corrections for the 1.5-caliber ogives are shown as a solid curve in figure B-1. We see that the wall-effect curves for the two nose shapes intersect in figure B-1. The blockage theory of Lock and Johansen[9] indicates that we may expect the correction curve for the ogives to have a slightly greater slope than the hemisphere correction curve, but certainly not an intersection as shown in figure B-1. It is estimated that the CIT values for the minimum C_p have a total uncertainty from all causes which is less than ±3 per cent. The precision of the Iowa data is not known.

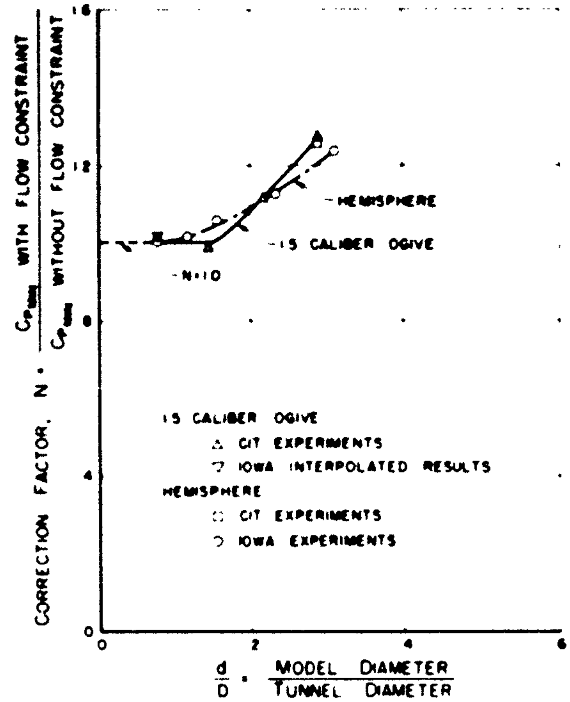

FIG. B-1 EXPERIMENTALLY DETERMINED BLOCKAGE CORRECTION FACTORS

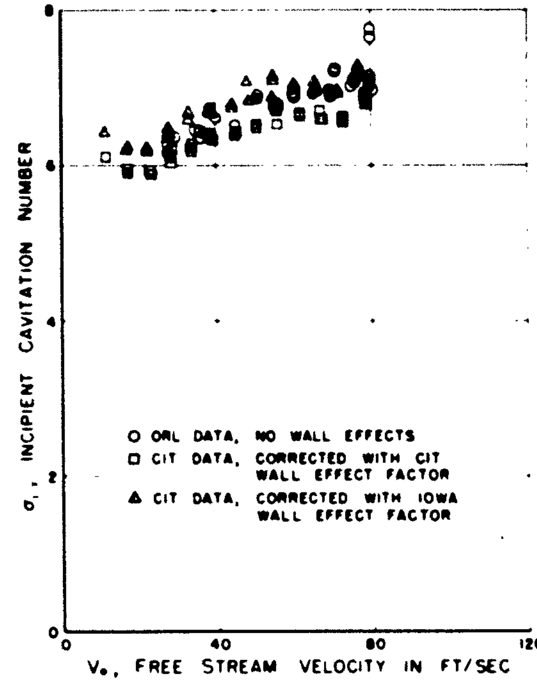

FIG. B-3 COMPARISON OF CIT AND ORL DATA FOR 4-INCH HEMISPHERE WITH IOWA AND CIT BLOCKAGE CORRECTIONS APPLIED TO CIT DATA

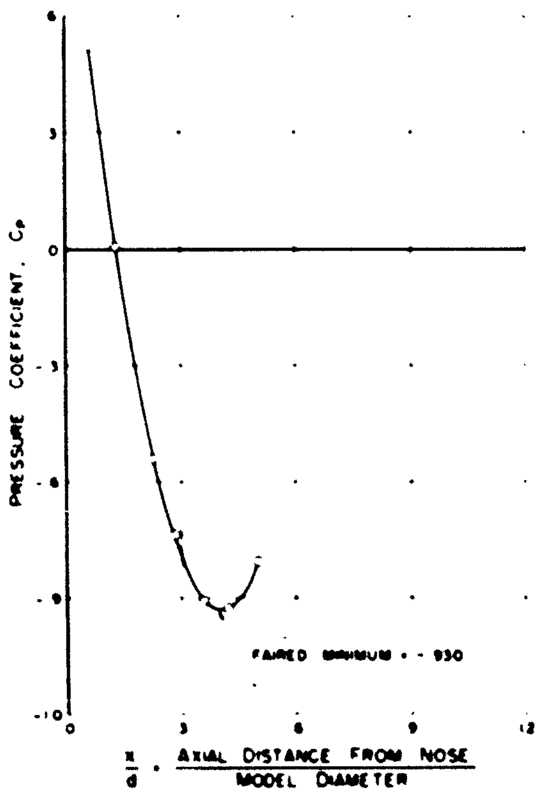

FIG. B-2 PRESSURE DISTRIBUTION AROUND 4-INCH HEMISPHERE NOSE IN THE HIGH-SPEED WATER TUNNEL

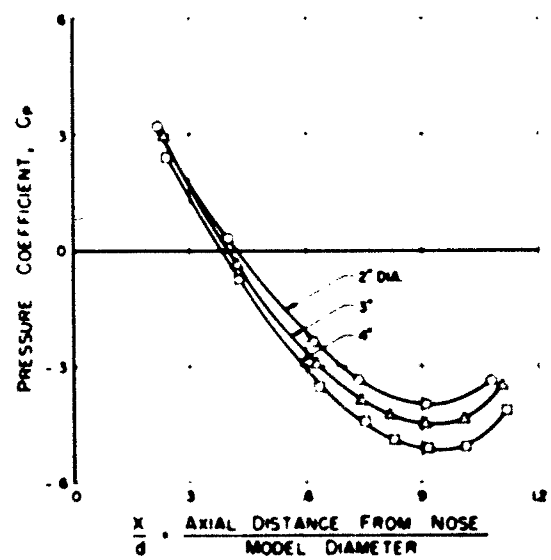

FIG. B-4 EFFECT OF TUNNEL WALLS UPON THE PRESSURE DISTRIBUTION OF 1.5-CALIBER OGIVE NOSES

Appendix C

Tables of Experimental Data

The attached tables give the values of the incipient cavitation numbers which were found from visual observations of the flow. The values given here have been corrected in accordance with the procedure outlined in the section entitled Reduction of Data, page 4.

1.4"-Diameter Hemisphere - August 8, 1952
O.R.L. Test No. 726

Time	σ_i	V_o	$V_o\sqrt{d}$	$R_e \times 10^{-5}$	Air Content* As Measured	Air Content* Corrected
1535					5.2	7.2
1553	.582	29.3	4.93	.803		
1555	.576	29.3	4.93	.803		
1616	.677	36.2	6.09	.990		
1618	.704	36.2	6.09	.990		
1620	.710	42.2	7.10	1.15		
1625	.670	42.2	7.10	1.15		
1627	.660	42.2	7.10	1.15		
1628	.629	46.1	7.76	1.26		
1632	.650	46.1	7.76	1.26		
1633	.632	50.9	8.56	1.40		
1634	.643	50.9	8.56	1.40		
1636	.620	55.2	9.29	1.51		
1638	.633	55.2	9.29	1.51		
1640	.616	60.6	10.2	1.66		
1643	.620	60.6	10.2	1.66		
1645	.604	70.1	11.8	1.92		
1647	.628	70.1	11.8	1.92		
1649	.619	70.1	11.8	1.92		
1651	.606	79.9	13.4	2.19	5.0	7.2
1652	.626	79.9	13.4	2.19		
1655					5.2	7.6

3.8"-Diameter Hemisphere - August 8, 1952
O.R.L. Test No. 726

Time	σ_i	V_o	$V_o\sqrt{d}$	$R_e \times 10^{-5}$	Air Content As Measured	Air Content Corrected
1547	.554	30.6	5.41	1.24		
1548	.554	30.6	5.41	1.24		
1550	.551	36.1	6.38	1.46		
1554	.558	36.1	6.38	1.46		
1555	.562	39.7	7.02	1.61		
1558	.561	39.7	7.02	1.61		
1611					4.1	7.0
1622	.560	45.9	8.12	1.86		
1625	.564	45.9	8.12	1.86		
1626	.566	50.4	8.91	2.04		
1627	.566	50.4	8.91	2.04		
1628	.572	55.6	9.83	2.25		
1631	.572	55.6	9.83	2.25		
1632	.574	59.7	10.6	2.42		
1634	.582	59.7	10.6	2.42		
1636	.594	64.7	11.4	2.62	5.6	7.6
1639	.594	64.7	11.4	2.62		
1640	.601	69.6	12.3	2.82		
1642	.601	69.6	12.3	2.82		
1644	.601	74.6	13.2	3.02		
1647	.610	74.6	13.2	3.02		
1649	.621	79.5	14.1	3.19		
1651	.621	79.5	14.1	3.19		
1655	.556	46.3	8.18	1.89		
1657	.562	46.3	8.18	1.89		
1659					5.6	7.9

* All air contents are in parts per million. The values of air content for the ORL tests were corrected to account for water vapor on the mercury column of the Van Slyke apparatus.

1/2"-Diameter Hemisphere - August 8, 1952
O.R.L. Test No. 725

Time	σ_i	V_o	$V_o\sqrt{d}$	$R_e \times 10^{-5}$	Air Content As Measured	Air Content Corrected
0954	.584	28.5	5.82	1.66		
0957	.584	28.5	5.82	1.66		
1011					3.7	7.5
1016	.535	32.4	6.61	1.71		
1018	.542	32.4	6.61	1.71		
1035					4.2	7.8
1039	.550	37.2	7.59	1.96		
1040	.550	37.2	7.59	1.96		
1042	.562	40.7	8.30	2.14		
1045	.550	40.7	8.30	2.14		
1100					3.7	7.4
1106	.580	46.8	9.55	2.47		
1108	.568	46.8	9.55	2.47		
1110	.574	50.5	10.3	2.66		
1111	.574	50.5	10.3	2.66		
1114	.583	55.2	11.3	2.90		
1116	.591	55.2	11.3	2.90		
1118	.600	60.4	12.3	3.19		
1120	.606	60.4	12.3	3.19		
1125	.619	65.0	13.3	3.42		
1125	.633	65.0	13.3	3.42		
1126	.600	70.1	14.3	3.69		
1126	.611	70.1	14.3	3.69		
1130	.626	70.1	14.3	3.69		
1133	.625	74.8	15.3	3.93		
1134	.632	74.8	15.3	3.93		
1136	.643	79.8	16.3	4.21		
1140	.644	79.8	16.3	4.21		
1140	.574	46.6	9.51	2.45		
1143	.577	46.6	9.51	2.45		

1-1/8"-Diameter Hemisphere - August 7-8, 1952
O.R.L. Tests Nos. 724 and 725

Test No. 724 -

Time	σ_i	V_o	$V_o\sqrt{d}$	$R_e \times 10^{-5}$	Air Content As Measured	Air Content Corrected
1510	.620	40.9	12.5	4.85	3.2	7.2
1518						
1521	.629	45.9	14.1	5.45		
1525	.646	49.8	15.2	5.91		
1530					3.1	7.1
1550	.647	55.0	16.8	6.53		
1601	.670	59.7	18.3	7.09		
1607	.656	65.0	19.9	7.72		
1610	.666	69.9	21.4	8.29		
1616	.670	75.0	23.0	8.89		
1619	.681	79.7	24.4	9.46		
1623	.680	79.7	24.4	9.46		
1624	.676	74.6	22.8	8.84		
1627	.679	74.6	22.8	8.84		
1628	.677	69.7	21.3	8.27		
1632	.680	69.7	21.3	8.27		
1636	.666	64.4	19.7	7.65	2.8	6.9
1638	.666	64.4	19.7	7.65		
1642	.653	59.5	18.2	7.06		
1643	.650	59.5	18.2	7.06		
1652					3.2	7.3

Test No. 725 -

Time	σ_i	V_o	$V_o\sqrt{d}$	$R_e \times 10^{-5}$	Air Content As Measured	Air Content Corrected
0822					4.7	8.1
0825	.590	36.4	11.1	4.31		
0840					4.7	8.2
0843	.590	32.1	9.81	3.81		
0857					4.3	7.8
0906	.570	26.1	7.99	3.10		
0907	.580	30.6	9.37	3.60		
0907	.580	30.6	9.37	3.60		
0908	.595	36.7	11.2	4.35		
0909	.596	36.7	11.2	4.35		
0911					3.9	7.5
0923					3.7	7.6

2"-Diameter Hemisphere - August 6-7, 1952
O.R.L. Tests Nos. 722, 723, 724

Test No. 722 -

Time	σ_i	V_o	$V_o\sqrt{d}$	$R_e \times 10^{-5}$	Air Content As Measured	Air Content Corrected
1320					3.2	6.8
1328	.614	31.5	12.9	6.49		
1346	.600	25.5	10.4	5.24		
1400					2.8	6.6
1413	.592	30.5	12.4	6.28		
1430					2.7	6.6
1434	.618	36.5	14.9	7.50		
1455					2.5	6.4
1521	.643	50.5	20.6	10.4	3.6	7.5
1528	.632	44.9	18.3	9.24	3.6	7.5
1550	.608	27.6	11.3	5.68	3.4	7.4
1605	.625	30.7	12.5	6.33		
1615					3.1	7.1
1623	.624	41.0	16.7	8.72		
1625	.652	54.8	22.4	11.3		
1631	.620	59.3	24.2	12.2		
1638	.668	65.0	26.5	13.4		
1643	.674	70.1	28.6	14.4		
1648	.682	74.6	30.4	15.3		
1651	.681	80.3	32.8	16.5		

Test No. 723 -

Time	σ_i	V_o	$V_o\sqrt{d}$	$R_e \times 10^{-5}$	Air Content As Measured	Air Content Corrected
0855	.632	40.9	16.7	8.42	4.8	7.8
0902	.641	45.1	18.4	9.28		
0908	.650	51.2	20.9	10.6		
0913	.656	55.8	22.8	11.5		
0919	.668	60.6	24.7	12.5		
0933	.664	60.8	24.8	12.5	4.1	7.3
0941	.677	65.0	26.5	13.4		
0947	.679	70.2	28.6	14.4		
0952	.677	75.0	30.6	15.4		
0956	.676	79.8	32.6	16.4		
1010					3.4	6.8
1055					3.7	7.2
1145					3.4	7.0

Test No. 724 -

Time	σ_i	V_o	$V_o\sqrt{d}$	$R_e \times 10^{-5}$	Air Content As Measured	Air Content Corrected
1330					4.2	7.7
1336	.606	24.0	9.79	4.94		
1355					3.9	7.6
1401	.618	31.2	12.7	6.42		
1410					3.6	7.4
1414	.612	36.5	14.9	7.50		
1430					3.56	7.4

6"-Diameter Hemisphere - August 12, 1952
O.R.L. Tests Nos. 729 and 730

Test No. 729 -

Time	σ_i	V_o	$V_o\sqrt{d}$	$R_e \times 10^{-5}$	Air Content As Measured	Air Content Corrected
0918					5.3	8.6
0924	.685	50.4	29.1	20.7		
0926	.690	50.4	29.1	20.7		
0927	.676	55.0	31.7	22.7		
0929	.678	55.0	31.7	22.7		
0930	.689	59.8	34.5	24.6		
0932	.693	59.8	34.5	24.6		
0934	.693	65.0	37.5	26.7		
0936	.693	65.0	37.5	26.7		
1002					4.6	8.1
1008	.724	70.5	40.7	29.0		
1010	.721	70.5	40.7	29.0		
1011	.708	75.6	43.6	31.1		
1013	.710	75.6	43.6	31.1		
1015	.703	79.3	45.7	32.6		
1017	.703	79.3	45.7	32.6		
1017	.680	55.6	32.0	22.7		
1022	.680	55.6	32.0	22.7		
1023	.680	55.6	32.0	22.7		
1025					5.0	8.5
1049					4.4	8.0
1053	.675	54.6	31.5	22.4		
1055	.677	54.6	31.5	22.4		
1056	.696	70.2	40.5	28.8		
1059	.696	70.2	40.5	28.8		
1101	.775	79.7	46.0	32.8		
1106	.764	79.7	46.0	32.8		
1107	.764	79.7	46.0	32.8		
1110					4.4	8.1
1115	.652	44.4	25.6	18.2		
1116	.652	44.4	25.6	18.2		
1118	.617	38.3	22.1	15.7		
1118	.672	38.3	22.1	15.7		
1121	.617	38.3	22.1	15.7		
1123	.641	38.3	22.1	15.7		
1151					4.2	8.0
Test No. 730						
1326					4.9	8.6
1332	.661	39.9	23.0	16.4		
1333	.661	39.9	23.0	16.4		
1336	.635	35.9	20.7	14.7		
1336	.646	35.9	20.7	14.7		
1336	.645	35.9	20.7	14.7		
1433	.627	27.0	15.6	11.0		
1433	.616	27.0	15.6	11.0		
1436					4.6, 4.5	8.4, 8.3 Nozzle
1436					4.2, 4.4	8.0, 8.3 Diffuser
1436					4.5, 4.3	8.3, 8.2 Lower Leg
1504	.636	29.8	16.7	11.9		
1505	.636	29.8	16.7	11.9		
1506	.665	34.6	20.0	14.2		
1509	.665	34.6	20.0	14.2		
1512	.696	69.7	40.2	28.6		
1516	.688	69.7	40.2	28.6		
1516	.694	69.7	40.2	28.6		
1520	.701	74.6	43.1	30.7		
1521	.701	74.6	43.1	30.7		
1523	.716	79.5	45.9	32.7		
1526	.708	79.5	45.9	32.7		

8"-Diameter Hemisphere - August 11, 1952
O.R.L. Tests Nos. 727 and 728

Test No. 727 -

Time	σ_i	V_o	$V_o\sqrt{d}$	$R_e \times 10^{-5}$	Air Content As Measured	Air Content Corrected
0916					5.7	8.6
1002					4.5	7.7
1012	.725	61.2	50.0	49.8		
1014	.730	61.2	50.0	49.8		
1016	.726	61.2	50.0	49.8		
1021	.737	65.4	53.4	53.2		
1022					4.6	8.0
1024	.734	65.4	53.4	53.2		
1026	.736	70.2	57.3	57.1		
1029	.738	70.2	57.3	57.1		
1030	.743	74.8	61.1	60.7		
1032	.743	74.8	61.1	60.7		
1034	.745	79.3	64.8	64.5		
1036	.739	79.3	64.8	64.5		
1106					4.2	7.7
1113	.732	55.2	45.1	44.9		
1113	.716	55.2	45.1	44.9		
1116	.718	55.2	45.1	44.9		
1118	.695	50.5	41.2	41.1		
1122	.694	50.5	41.2	41.1		
1123	.695	50.5	41.2	41.1		
Test No. 728 -						
1130					4.2	7.7
1132	.737	79.7	65.1	64.8		
1135	.740	79.7	65.1	64.8		
1140	.672	44.5	36.3	36.3		
1142	.680	44.5	36.3	36.3		
1144	.703	40.1	32.7	32.6		
1145	.703	40.1	32.7	32.6		
1147	.693	40.1	32.7	32.6		
1149	.682	33.8	27.6	27.5		
1151	.671	33.8	27.6	27.5		
1350					4.3	8.0
1356	.670	32.6	26.6	26.5		
1357	.664	32.6	26.6	26.5		
1415					3.8	7.6
1422	.664	24.3	19.8	19.8		
1453					4.0	7.9
1511	.688	23.4	19.1	19.0		
1528	.646	24.9	20.6	20.2	3.7	7.7
1551	.670	26.3	21.5	21.4		
1553	.693	46.1	37.6	37.5		
1555	.696	46.1	37.6	37.5		
1557	.747	48.0	39.2	39.0		
1557	.766	48.0	39.2	39.0		
1605					3.6	7.6
1613	.688	50.1	40.9	40.7		
1615	.686	50.1	40.9	40.7		
1624	.680	54.6	44.6	44.4		
1624	.687	54.6	44.6	44.4		
1627	.700	59.6	48.7	48.5		
1627	.698	59.6	48.7	48.5		
1633	.668	44.6	36.4	36.3		
1633	.678	44.6	36.4	36.3		
1635					4.8	8.1

1/4"-Diameter Hemisphere "A"*

σ_i	V_o	$R_e \times 10^{-5}$	$V_o\sqrt{d}$	Dissolved Air Content P.P.M.	Water Temp °F	Run
.665	30.2	.776	5.00	7.61	91.4	16
.667	30.2	.776	5.00			"
.500	36.0	.896	5.86		91.6	"
.500	36.0	.896	5.86			"
.559	39.5	1.02	6.65			"
.506	39.5	1.02	6.65			"
.562	44.7	1.15	7.51			"
.561	44.7	1.15	7.51			"
.560	44.0	1.13	7.53		89.6	"
.565	44.0	1.13	7.53			"
.501	49.7	1.27	8.37		91.0	"
.602	55.1	1.41	9.27	7.24		"
.617	59.5	1.52	10.0		91.4	"
.625	65.1	1.60	11.0		91.8	"
.621	70.4	1.81	11.8		92.0	"
.637	75.7	1.97	12.7		92.6	"
.662	79.3	2.09	13.3		93.0	"
.654	84.7	2.23	14.3		93.2	"
.652	84.5	2.22	14.2	7.24	93.0	17
.652	84.5	2.22	14.2			"
.651	75.7	2.30	12.7		93.8	"
.647	75.7	2.30	12.7			"
.628	64.9	1.72	10.9		94.0	"
.636	64.9	1.72	10.9			"
.622	64.9	1.72	19.9			"
.620	64.9	1.72	10.9			"
.600	55.2	1.47	9.28		94.2	"
.609	55.2	1.47	9.28			"
.575	44.8	1.19	7.54		94.3	"
.565	44.8	1.19	7.54			"
.512	35.0	.912	5.88		94.3	"
.517	35.0	.912	5.88			"
.607	24.3	.646	4.28		94.3	"
.600	24.3	.646	4.28			"
.640	59.5	1.21	10.0			32
.704	49.6	1.01	8.34			32
.609	49.6	1.01				32
.557	39.6	0.81	6.66			32
.629	39.6	0.81	6.66			32
.619	29.7	0.61	4.99			32
[illegible]	29.7	0.61	4.99			32

* Data from R. W. Kermeen[2] This data was taken during the period April 1951 to January 1952

1/2"-Diameter Hemisphere "B"*

σ_i	V_o	$R_e \times 10^{-5}$	$V_o\sqrt{d}$	Dissolved Air Content P.P.M.	Water Temp. °F	Run
.776	20.4	1.03	4.16	7.7	90.0	16
.846	20.4	1.03	4.16			"
.793	20.4	1.03	4.16			"
.697	24.2	1.22	4.94			"
.684	24.2	1.22	4.94			"
.652	30.7	1.55	6.27			"
.608	30.7	1.55	6.27			"
.571	30.7	1.55	6.27			"
.623	30.7	1.55	6.27			"
.560	34.7	1.75	7.08			"
.559	34.7	1.75	7.08			"
.600	38.6	1.95	7.88		90.0	"
.591	38.6	1.95	7.88			"
.591	38.6	1.95	7.88			"
.591	44.7	2.26	9.10			"
.594	44.7	2.26	9.10			"
.580	44.7	2.26	9.10			"
.597	44.7	2.26	9.10			"
.623	48.9	2.47	9.98		90.2	"
.620	48.9	2.47	9.98			"
.624	54.2	2.75	11.1		90.4	"
.623	54.2	2.75	11.1			"
.630	58.7	2.98	12.0			"
.626	58.7	2.98	12.0			"
.629	58.7	2.98	12.0			"
.608	64.9	3.28	13.2			"
.637	64.9	3.28	13.2			"
.633	64.9	3.28	13.2			"
.635	70.0	3.57	14.3		90.6	"
.637	70.0	3.57	14.3			"
.640	69.9	3.52	14.2		90.6	"
.633	75.8	3.86	15.5	7.3		"
.649	79.5	4.07	16.2		91.0	"
.662	84.6	4.34	17.3		91.4	"
.654	59.4	3.05	12.1	7.7	91.6	15
.622	59.4	3.05	12.1			"
.607	49.6	2.55	10.2		91.8	"
.597	49.6	2.55	10.2			"
.566	39.4	2.03	8.04		91.8	"
.574	39.4	2.03	8.04			"
.520	30.2	1.56	6.16			"
.519	30.2	1.56	6.16			"

* Data from R. W. Kermeen[2] This data was taken during the period April 1951 to January 1952

3/8"-Diameter Hemisphere*

σ_i	V_o	$R_e \times 10^{-5}$	$V_o\sqrt{d}$	Dissolved Air Content P.P.M.	Water Temp °F	Run
.552	30.0	.88	5.50	6.0	69.6	26
.522	40.1	1.16	7.34			"
.557	50.1	1.47	8.85		69.7	"
.592	60.2	1.77	10.6			"
.567	55.2	1.62	9.75			"
.759	30.1	.88	5.56	7.5	71.2	27
.560	25.0	.75	4.42			"
.566	25.0	.75	4.42			"
.566	25.0	.75	4.42			"
.661	29.9	.94	5.29		71.3	"
.611	29.9	.94	5.29			"
.713	29.9	.94	5.29			"
.521	35.0	1.05	6.17		71.4	"
.566	35.2	1.05	6.17			"
.562	39.9	1.20	7.06		71.5	"
.536	39.9	1.20	7.06			"
.557	45.0	1.36	7.95		71.6	"
.560	45.0	1.36	7.95			"
.571	50.0	1.50	8.86		71.7	"
.573	50.0	1.50	8.86			"
.583	55.0	1.67	9.72		71.8	"
.576	55.0	1.67	9.72			"
.594	60.0	1.82	10.6			"
.590	60.0	1.82	10.6			"
.640	65.6	2.00	11.6	7.5	72.6	28
.613	65.3	2.00	11.5			"
.667	65.3	2.00	11.5			"
.646	70.2	2.15	12.4			"
.600	70.2	2.15	12.4			"
.629	75.1	2.31	13.4			"
.627	75.1	2.31	13.4			"
.637	80.1	2.46	14.2			"
.666	90.1	2.77	16.0			"

* Data from R. W. Kermeen[2] This data was taken during the period April 1951 to January 1952

1-1/4"-Diameter Hemisphere*

σ_i	V_o	$R_e \times 10^{-5}$	$V_o\sqrt{d}$	Dissolved Air Content P.P.M.	Water Temp. °F	Run
.592	15.6	1.69	4.72	7.5	87.0	11
.571	15.6	1.69	4.72			"
.613	20.6	2.24	6.25			"
.641	20.6	2.24	6.25			"
.651	20.6	2.24	6.25			"
.585	24.6	2.67	7.45			"
.616	30.1	3.30	8.56			"
.632	34.9	3.83	10.7			"
.663	39.6	4.31	12.0			"
.661	39.6	4.31	12.0			"
.652	44.7	4.91	13.7			"
.676	49.6	5.45	15.2			"
.672	54.9	6.03	16.8		87.2	"
.696	59.7	6.56	18.3	7.7	87.4	"
.696	65.0	7.06	19.9		87.8	"
.702	69.8	7.76	22.4		88.0	"
.715	75.7	8.41	23.2		88.2	"
.713	79.5	8.87	24.2		88.8	"
.716	84.7	9.32	25.9		89.0	"

* Data from R. W. Kermeen[2] This data was taken during the period April 1951 to January 1952.

2" Smooth Hemisphere "B" *

e_i	V_o	$R_e \times 10^{-5}$	$V_o\sqrt{d}$	Dissolved Air Content P.P.M.	Water Temp. °F	Run
765	84.7	16.93	34.6	8.6	89.6	10
.723	84.7	16.93	34.6			"
.723	84.7	16.93	34.6			"
.704	75.0	15.27	30.9			"
.691	75.0	15.27	30.9			"
.703	64.9	13.09	26.4		90.0	"
.703	64.9	13.09	26.4			"
689	55.2	11.05	22.5		89.3	"
.690	55.2	11.05	22.5			"
.669	44.8	8.98	18.3			"
.670	44.8	8.98	18.3			"
650	35.0	7.01	14.3			"
655	35.0	7.01	14.3			"
595	24.5	4.96	10.0		90.2	"
.601	24.5	4.96	10.0			"
517	15.5	3.14	6.34			"
519	15.5	3.14	6.34			"

* Data from R. W. Kermeen[2]. This data was taken during the period April 1951 to January 1952

1/2"-Diameter 1.5-Calibre Ogive - August 14, 1952
O.R.L. Test No. 735

Time	e_i	V_o	$V_o\sqrt{d}$	$R_e \times 10^{-5}$	Air Content As Measured	Air Content Corrected
1330					4.0	7.6
1405					3.6	7.1
1414	.191	42.9	8.76	2.39		
1416	.191	42.9	8.76	2.39		
1422	.193	46.5	9.48	2.58		
1423	.193	46.5	9.48	2.58		
1430	.202	50.5	10.3	2.81		
1430	.202	50.5	10.3	2.81		
1433	.212	54.6	11.1	3.04		
1434	.216	54.6	11.1	3.04		
1438	.226	59.6	12.2	3.31		
1440	.223	59.6	12.2	3.31		
1442	.229	64.5	13.2	3.59		
1444	.228	64.5	13.2	3.59		
1446	.234	69.6	14.2	3.87		
1448	.238	69.6	14.2	3.87		
1450	.230	74.4	15.2	4.13		
1452	.233	74.4	15.2	4.13		
1455	.236	79.5	16.2	4.42		
1455	238	79.5	16.2	4.42		
1519					4.5	8.3

4"-Diameter Hemisphere - October 16, 1952
C.I.T. Test

e_i	V_o	$R_e \times 10^{-5}$	$V_o\sqrt{d}$	Dissolved Air Content P.P.M.
695	65.4	24.6	37.8	Av 9.0
707	65.1	24.4	37.6	
702	65.6	24.7	37.8	
705	59.8	22.6	34.6	
.703	59.9	22.6	34.6	
.710	54.3	20.4	31.4	
.716	54.1	20.4	31.2	
690	54.4	20.5	31.4	
.700	54.4	20.5	31.4	
700	47.9	18.5	27.6	
685	48.2	18.6	27.8	
677	43.0	16.5	25.1	
680	43.0	16.5	25.1	
680	43.0	16.5	25.1	
660	38.2	14.4	22.0	
.671	38.0	14.4	21.9	
660	32.8	12.3	18.9	
660	32.8	12.4	18.9	
.666	32.7	12.3	18.9	
669	27.4	10.4	15.8	
659	27.4	10.4	15.8	
.661	27.3	10.4	15.8	
686	21.8	8.3	12.6	
.686	21.8	8.3	12.6	
682	21.8	8.3	12.6	
.649	16.5	6.3	9.5	
.646	16.5	6.3	9.5	
.666	10.8	4.1	6.2	
690	71.0	27.0	41.0	
695	71.0	27.0	41.0	
696	71.0	27.0	41.0	
715	76.4	30.2	44.1	
.715	76.4	30.2	44.1	
.718	76.4	30.2	44.1	
780	76.4	30.2	44.1	
.780	76.4	30.2	44.1	

1"-Diameter 1.5-Calibre Ogive - August 14, 1952
O.R.L. Test No. 734

Time	e_i	V_o	$V_o\sqrt{d}$	$R_e \times 10^{-5}$	Air Content As Measured	Air Content Corrected
0837					5.2	8.1
1102					4.6	7.8
1105	.223	50.8	14.6	5.52		
1106	.227	50.8	14.6	5.52		
1109	.235	55.0	15.9	5.97		
1110	.233	55.0	15.9	5.97		
1112	.240	59.4	17.1	6.44		
1114	.238	59.4	17.1	6.44		
1115	.247	64.6	18.6	7.01		
1116	.250	64.6	18.6	7.01		
1119	.251	69.8	20.1	7.56		
1120	.251	69.8	20.1	7.56		
1122	.257	75.6	21.8	8.29		
1124	.259	75.6	21.8	8.29		
1126	.262	79.6	23.0	8.62		
1127	.262	79.6	23.0	8.62		
1131	226	44.8	12.9	4.85		
1132	.222	44.8	12.9	4.85		
1136	.215	40.6	11.7	4.40		
1137	.215	40.6	11.7	4.40		
1144					4.5	7.8

2"-Diameter 1.5-Calibre Ogive - August 13, 1952
O.R.L. Test No. 733

Time	e_i	V_o	$V_o\sqrt{d}$	$R_e \times 10^{-5}$	Air Content As Measured	Air Content Corrected
1507					6.3	8.6
1513	.260	45.0	18.4	10.00		
1520	.265	45.0	18.4	10.00		
1528	.267	50.1	20.4	11.2		
1531	.262	50.1	20.4	11.2		
1536	.269	55.0	22.4	12.3		
1543	.264	55.0	22.4	12.3		
1545	.275	59.8	24.4	13.4		
1547	.284	59.8	24.4	13.4		
1549	.275	64.6	26.4	14.4		
1551	275	64.6	26.4	14.4		
1553	291	69.9	28.5	15.7		
1555	.291	69.9	28.5	15.7		
1558	.301	74.8	30.5	16.00		
1559	.299	74.8	30.5	16.00		
1602	.310	79.3	32.4	17.00		
1603	.316	79.3	32.4	17.00		
1608					6.1	7.8

4"-Diameter 1.5-Calibre Ogive - August 13, 1952
O.R.L. Tests Nos. 731 and 732

Test No. 731

Time	σ_i	V_o	$V_o\sqrt{d}$	$R_e \times 10^{-5}$	Air Content As Measured	Air Content Corrected
0904					4.6	7.8
0925	.310	49.9	28.8	21.1		
0942	300	49.9	28.8	21.1		
0950	.312	55.2	31.8	23.3		
1006	.314	55.2	31.8	23.3		
1020					4.3	7.6
1026	.317	59.6	34.4	25.2		
1031	.323	59.6	34.4	25.2		
1038	.324	64.7	37.3	27.3		
1045	.329	64.7	37.3	27.3		
1055	.330	70.0	40.4	29.5		
1103	330	70.0	40.4	29.5		
1110					3.9	7.5
1112	336	74.7	43.1	31.5		
1120	336	74.7	43.1	31.5		
1130	.338	79.3	45.8	33.5		
1138	.334	79.3	45.8	33.5		
1141					3.6	7.3
1144	.298	49.8	28.7	21.0		
1146	293	49.8	28.7	21.0		

Test No. 732

Time	σ_i	V_o	$V_o\sqrt{d}$	$R_e \times 10^{-5}$	Air Content As Measured	Air Content Corrected
1332					4.3	7.9
1336	286	45.9	26.5	19.4		
1340	278	45.9	26.5	19.4		
1346	286	45.9	26.5	19.4		
1357					4.0	7.7
1416					4.0	7.7

1.2"-Diameter 1.5-Calibre Ogive - October 15, 1952
C.I.T. Test

σ_i	V_o	$R_e \times 10^{-5}$	$V_o\sqrt{d}$	Air Content
.266	100.4	4.75	20.5	8.5 P.P.M.
.265	100.4	4.75	20.5	
.268	100.4	4.75	20.5	
257	90.2	4.26	18.4	
265	90.2	4.26	18.4	
261	90.2	4.26	18.4	
.256	85.2	4.03	17.4	
.259	85.2	4.03	17.4	
264	85.2	4.03	17.4	
.258	85.2	4.03	17.4	
255	80.1	3.79	16.3	
258	80.1	3.79	16.3	
256	80.1	3.79	16.3	
267	75.2	3.56	15.3	
252	75.2	3.56	15.3	
.260	75.2	3.56	15.3	
.269	70.1	3.32	14.3	
.252	70.1	3.32	14.3	
267	70.1	3.32	14.3	
.236	65.1	3.08	13.3	
262	65.1	3.08	13.3	
.262	65.1	3.08	13.3	
.239	59.8	2.83	12.2	
.227	59.7	2.82	12.2	
.226	59.9	2.83	12.2	
.225	55.1	2.61	11.2	
226	55.1	2.61	11.2	
220	50.0	2.36	10.2	
.218	50.0	2.37	10.2	
218	50.1	2.37	10.2	
.199	44.8	2.12	9.14	
.207	44.9	2.12	9.16	
206	44.9	2.12	9.16	
.211	39.7	1.88	8.10	
.198	40.0	1.89	8.16	
.197	40.0	1.89	8.16	
188	34.8	1.64	7.10	
189	34.8	1.64	7.10	
.210	29.9	1.41	6.10	
.171	29.8	1.41	6.08	
.170	29.8	1.41	6.08	

1"-Diameter 1.5-Calibre Ogive - October 8-14, 1952
C.I.T. Test

σ_i	V_o	$R_e \times 10^{-5}$	$V_o\sqrt{d}$	Air Content
.216	29.7	2.72	8.56	
.221	29.7	2.72	8.56	
.219	34.6	3.17	9.98	
.219	34.7	3.18	10.0	
.227	39.7	3.64	11.4	
.225	39.7	3.63	11.4	
.232	44.6	4.09	12.9	
.232	44.6	4.08	12.9	
.240	49.6	4.54	14.3	
.245	49.8	4.56	14.4	
.244	49.6	4.55	14.3	
.243	54.7	5.01	15.8	
.243	54.5	4.99	15.7	
.248	59.3	5.43	17.1	
.246	59.5	5.44	17.2	
.254	64.7	5.92	18.7	
.251	64.7	5.92	18.7	
.248	65.1	5.96	18.8	
.255	65.1	5.96	18.8	
.252	65.1	5.96	18.8	7.4 Av.
.287	97.4	8.92	28.1	
.283	97.4	8.92	28.1	
.277	90.2	8.26	26.0	
.277	90.2	8.26	26.0	
.276	85.3	7.81	24.6	
.278	85.3	7.81	24.6	
.274	80.2	7.35	23.2	
.274	80.2	7.35	23.2	
.274	75.3	6.90	21.7	
.276	75.3	6.90	21.7	
.269	70.2	6.43	20.3	6.2
.270	70.2	6.43	20.3	
.263	65.4	5.99	18.9	
.265	65.4	5.99	18.9	
.265	60.2	5.52	17.4	
.238	30.0	2.75	8.65	
.231	29.9	2.74	8.62	
.256	40.1	3.67	11.6	
.249	40.0	3.67	11.5	
.228	24.4	2.26	7.04	11.0 Av.
.237	29.0	2.68	8.36	
.238	28.9	2.67	8.34	
.224	30.0	2.78	8.65	
.220	29.9	2.77	8.63	
.228	35.1	3.24	10.1	
.232	34.9	3.22	10.1	
.238	40.0	3.70	11.5	
.235	40.1	3.71	11.6	
.248	45.1	4.17	13.0	
.246	44.9	4.15	13.0	
.248	45.0	4.16	13.0	
.255	50.1	4.63	14.4	
.258	50.0	4.62	14.4	
.257	55.0	5.08	15.9	
.256	55.0	5.08	15.9	
.257	60.1	5.56	17.3	
.260	60.1	5.56	17.3	
.261	60.1	5.55	17.3	12.3
.284	65.2	6.15	18.8	"
.283	65.2	6.15	18.8	"
.279	65.2	6.15	18.8	"
.285	70.0	6.61	20.2	"
.281	70.0	6.61	20.2	"
.279	70.0	6.61	20.2	"
.278	75.2	7.10	21.7	8.5
.274	75.2	7.10	21.7	"
.278	75.2	7.10	21.7	"
.276	80.2	7.57	23.2	"
.273	80.2	7.57	23.2	"
.282	80.2	7.57	23.2	"
.276	85.2	8.04	24.6	"

1"-Diameter 1.5-Calibre Ogive - October 8-14, 1952
C.I.T. Test (Continued)

σ_i	V_o	$R_e \times 10^{-5}$	$V_o\sqrt{d}$	Air Content
.280	85.2	8.04	24.6	8.9
.303	98.9	9.33	28.6	"
.291	98.9	9.33	28.6	"
.290	98.9	9.33	28.6	"
.294	98.6	9.28	28.5	"
.290	98.6	9.28	28.5	"
.273	90.3	8.50	26.0	"
.276	90.3	8.50	26.0	"
.273	90.3	8.50	26.0	"
.212	24.7	2.32	7.13	"
.223	24.7	2.32	7.13	"
.204	25.1	2.36	7.24	"
.213	30.0	2.82	8.65	"
.229	30.0	2.82	8.65	"
.228	30.0	2.82	8.65	"
.230	35.1	3.30	10.1	"
.232	35.1	3.31	10.1	"
.243	40.0	3.77	11.5	"
.243	40.2	3.79	11.6	"
.241	40.2	3.78	11.6	"
.249	45.2	4.25	13.0	"
.256	45.1	4.25	13.0	"
.262	49.8	4.69	14.4	"
.260	50.2	4.73	14.5	"
.260	50.1	4.72	14.5	"
.259	55.1	5.19	15.9	"
.259	55.2	5.19	15.9	"
.272	59.6	5.61	17.2	"
.264	59.9	5.64	17.3	"
.269	60.0	5.65	17.3	"

2"-Diameter 1.5-Calibre Ogive - October 15, 1952
C.I.T. Test (continued)

σ_i	V_o	$R_e \times 10^{-5}$	$V_o\sqrt{d}$	Air Content
.232	30.0	5.71	12.3	8.6
.239	25.1	4.78	10.2	"
.236	25.0	4.76	10.2	"
.240	25.0	4.76	10.2	"
.250	19.5	3.71	7.96	"
.229	19.6	3.73	8.00	"

2"-Diameter 1.5-Calibre Ogive - October 15, 1952
C.I.T. Test

σ_i	V_o	$R_e \times 10^{-5}$	$V_o\sqrt{d}$	Air Content
.319	103.3	19.61	42.1	8.6
.310	103.3		42.1	"
.316	103.3		42.1	"
.310	90.2	17.00	36.8	"
.307	90.2	17.00	36.8	"
.312	90.2	17.00	36.8	"
.311	84.9	16.00	34.6	"
.303	84.9	16.00	34.6	"
.302	84.9	16.00	34.6	"
.300	80.3	15.1	32.8	"
.299	80.3	15.1	32.8	"
.300	80.3	15.1	32.8	"
.297	75.2	14.2	30.7	"
.296	75.2	14.2	30.7	"
.300	75.2	14.2	30.7	"
.298	70.2	13.2	28.6	"
.296	70.2	13.2	28.6	"
.291	70.2	13.2	28.6	"
.294	65.2	12.4	26.6	"
.297	65.2	12.4	26.6	"
.297	65.2	12.4	26.6	"
.300	60.1	11.4	24.6	"
.291	60.0	11.4	24.4	"
.294	60.0	11.4	24.4	"
.282	56.1	10.5	22.9	"
.289	56.1	10.5	22.9	"
.288	55.9	10.6	22.8	"
.280	50.0	9.60	20.4	"
.280	50.0	9.52	20.4	"
.276	45.0	8.56	18.4	"
.272	45.0	8.56	18.4	"
.269	40.8	7.57	16.3	"
.268	40.0	7.61	16.3	"
.261	35.0	6.66	14.3	"
.260	34.9	6.64	14.3	"
.261	30.0	5.71	12.3	"

4"-Diameter 1.5-Calibre Ogive - October 16, 1952
C.I.T. Test

σ_i	V_o	$R_e \times 10^{-5}$	$V_o\sqrt{d}$	Air Content
.328	67.0	25.4	38.6	9.0
.323	67.0	25.4	38.6	
.331	67.0	25.2	38.6	
.325	62.0	23.4	35.8	
.319	61.8	23.3	35.6	
.336	61.4	23.2	35.4	
.319	61.8	23.3	35.6	
.331	55.1	21.2	31.8	
.330	55.0	21.2	31.7	
.330	55.0	21.2	31.7	
.321	50.5	19.0	29.2	
.322	50.4	19.0	29.1	
.315	50.3	19.0	29.0	
.320	50.5	19.0	29.2	
.307	44.9	17.0	25.9	
.306	45.1	17.0	26.0	
.296	44.7	16.9	25.8	
.289	44.8	16.9	25.8	
.298	44.8	16.9	25.8	
.315	44.8	16.9	25.8	
.298	39.1	14.9	22.6	
.304	39.2	14.9	22.6	
.295	39.2	14.9	22.6	
.296	39.2	14.9	22.6	
.279	33.7	12.7	19.4	
.286	33.7	12.7	19.4	
.284	33.6	12.7	19.4	
.283	33.6	12.7	19.4	
.299	28.2	10.7	16.3	
.286	28.1	10.6	16.2	
.280	28.1	10.6	16.2	
.277	28.2	10.7	16.3	
.282	28.0	10.6	16.2	
.284	21.8	8.3	12.6	
.286	22.1	8.3	12.8	
.280	22.1	8.3	12.8	

References

1. Parkin, Blaine R. Scale Effects in Cavitating Flow - A Preliminary Report. Report 21-7, Hydrodynamics Laboratory, CIT, December 28, 1951.

2. Kermeen, R. W. Some Observations of Cavitation on Hemispherical-Head Models. Report E-35.1, Hydrodynamics Laboratory, CIT, June 1952.

3. Parkin, Blaine R. Scale Effects in Cavitating Flow. Report 21-8, Hydrodynamics Laboratory, CIT, July 31, 1952.

4. Brown, F. Barton. Air Resorption in Water Tunnels. Report N-62, Hydrodynamics Laboratory, CIT, March 1949.

5. Power, R. B., Robertson, J. M., Ross, Donald, and Water Tunnel staff. Garfield Thomas Water Tunnel Operation. ORL report NOrd 7958-211, May 1, 1951.

6. Rouse, H., McNown, J. S., and Hsu, E. Summary of Cavitation Tests on a Systematic Series of Round Torpedo Heads. Final Report - Contract OEMsr 1353 (Declassified), Iowa Institute of Hydraulic Research, State University of Iowa, Iowa City, May 31, 1945, or
Rouse, H., and McNown, J. S. Cavitation and Pressure Distribution - Head Forms at Zero Angle of Yaw. Bulletin 32, State University of Iowa, Studies in Engineering.

7. Rouse, H. Engineering Hydraulics. John Wiley and Sons, 1950, page 1011.

8. McNown, J. S., and Lamb, C. A. Cavitation Tests on a Systematic Series of Torpedo Heads - Effect of Model Size. Report 14, Iowa Institute of Hydraulic Research, State University of Iowa, Iowa City, April 1947.

9. Lock, C. N. H., and Johansen, F. C. Wind-Tunnel Interference on Streamline Bodies. R and M 1451, Aeronautical Research Committee, 1931.